

HADRONIC FRAGMENTATION INITIATED BY POINTLIKE PROBES*

Thomas A. DeGrand
Stanford Linear Accelerator Center
Stanford University, Stanford, California 94305

ABSTRACT

Isotopic ratios of fast mesons produced in the target fragmentation region in reactions initiated by pointlike probes should resemble those seen in ordinary hadronic reactions when the probe removes sea partons from the target but should show dramatic changes once the probe knocks out valence partons. We use simple parton fusion models to predict the shapes and magnitudes of inclusive meson spectra (π^+ , π^- , K^+ , K^-) in the target fragmentation region of μp , νp and $\bar{\nu} p$ semiinclusive scattering and in the inclusive production of mesons in association with a massive lepton pair: $pp \rightarrow \mu^+ \mu^- MX$ or $p\bar{p} \rightarrow \mu^+ \mu^- MX$. Our predictions are in agreement with the limited existing data on these reactions and indicate areas where experiments may shed light on the correlated distribution of several partons in the nucleon.

(Submitted to Phys. Rev. D.)

*Work supported by the Department of Energy.

I. INTRODUCTION

Consider the archetype of a reaction induced by a pointlike probe: the scattering of a virtual photon γ^* and a proton, with subsequent production of hadrons. The hadronic single-particle inclusive spectrum will show a rapidity distribution similar to that of Fig. 1, with at least three distinct regions¹:

1. Particles moving rapidly along the photon's direction of motion arise from the fragmentation of a quark which the photon has knocked out of the proton and which follows the photon's line of motion. The distribution of particles in this region is similar to that seen in the reaction $e^+e^- \rightarrow q\bar{q} \rightarrow \text{hadrons}$.

2. Particles which follow the direction of the target particle lie in the target fragmentation region and arise from the "dressing-up" into hadrons of a system of partons from which one parton has been removed. The dynamics of the reaction should be similar to those of a purely hadronic reactions, which is also induced by the interaction of partons, although there the knocked-out parton is wee rather than of finite x .

3. Particles moving slowly with respect to the center-of-mass lie in the central region. Their distribution is essentially flat in rapidity. The central region may show a break in the region of phase space formerly occupied by the struck parton before it was removed (the "hole fragmentation region") if fragmentation of soft hadrons from the quark involves fundamentally different dynamics than does fragmentation of soft hadrons from the core.

Since the γ^*p reaction is initiated in the same way as an ordinary hadronic reaction, by the removal of a parton from the proton, the most

conservative phenomenological prediction for hadronic spectra in the target fragmentation region is that the shape of the spectrum should resemble the spectra seen in the target fragmentation region of ordinary hadronic reactions.

This expectation is born out by the data, where one observes

$$\frac{dN}{dx} \sim (1-x)^{3-4}$$

for the inclusive π^- spectrum as observed in the purely hadronic reaction $pN \rightarrow \pi X$ (Ref. 2), and in $\bar{\mu}p \rightarrow \mu^- \pi^- X$ (Ref. 3), and $\bar{\nu}p \rightarrow \mu^+ \pi^- X$ (Ref. 4), where x is a generic for an appropriate scaling variable (which will be discussed below).

However, there are important differences between purely hadronic and pointlike-induced reactions.

First, purely hadronic interactions are initiated by interactions among wee partons which are essentially independent of the flavor quantum numbers of the partons, so that particle spectra produced from the fragmentation of a given beam on a target are independent of the target. In deep-inelastic scattering the parton interaction which initiates the reaction depends on the flavor structure of the current, so that details of spectra--typically isotopic ratios of fast mesons--can vary from reaction to reaction depending on the preferred quark structure of the core which is left behind after the interaction.

Second, purely hadronic reactions are initiated by the interactions of wee hadrons, while in deep-inelastic scattering the interacting parton may be wee or fast, depending on the value of x_{Bj} selected by the lepton trigger. By virtue of the ability of the pointlike trigger to "remove" partons of varying x_{Bj} from the nucleon, changing x_{Bj} can have a dramatic and readily observable effect on single-particle inclusive spectra.

In the language of Bjorken,¹ these changes occur because the hole fragmentation region merges with the target fragmentation region, tangling quantum number effects of both regions.

In this paper we will explore parton model predictions for single meson inclusive spectra in the target fragmentation region in deep-inelastic and Drell-Yan induced scattering. We will present predictions based on two different parton models, one a model which has been applied with good success to a description of hadron-hadron single particle inclusive scattering,⁵ and the other a model based on a Bethe-Salpeter approach to fragmentation.⁶ This approach will prove useful in showing which predictions are more model independent and which predictions will be useful in differentiating one model from another. Throughout the paper, the aim will be to present predictions which are as conservative as possible, and which are based as much as possible on hadronic data.

The calculations of this paper do not bear any direct relation to the idea of charge retention, which is the study of the way in which flavor quantum numbers of jets should reflect the flavor quantum numbers of the quark or multiquark system which initiates the jet.⁷ For instance, the forward jet in the deep inelastic reaction $\bar{\nu}_p \rightarrow \mu^+ \text{jet } X$ at large x_{Bj} begins life as a d quark and should have a charge of roughly $-1/3$, modulo a universal constant. Charge retention is a global quantity, measured by summing over all the particles in the jet. This paper is concerned with single particle spectra, quantities which are local in x_F^* , the fraction of momentum in the jet carried by a single hadron. In principle, if one knew how to compute spectra for all mesons and baryons, including the effects of resonances, one could combine all the single particle

spectra into which the original jet constituents could evolve, suitably weighted by the appropriate quantum numbers such as charge or strangeness, and by brute force calculate the distribution of charge or strangeness in the jet as a function of x_F^* . The integrals of these distributions would yield the parameters associated with models of charge retention, such as the mean charge of the d quark jet just mentioned. That problem is too complicated to carry out at present without the use of an excessive number of parameters. To predict the magnitude of charge retention would, of course, be a goal in the further development of these models.

We briefly outline the remainder of the paper. In Section II we introduce our two parton models and discuss their similarities and differences. Section III is devoted to a discussion of semiinclusive deep-inelastic scattering in the target fragmentation region. Section IV contains our predictions for hadronic fragmentation accompanied by a massive dilepton pair, which has been discussed already elsewhere⁸ in less detail. Finally, our conclusions are tabulated in Section V.

II. FRAGMENTATION MODELS

We begin our study of semiinclusive scattering by discussing the models we will use. It will be important to present several complementary models which have rather different theoretical underpinning and yet purport to describe the data: that way, one will be able to make predictions about the data which are supported by several models and hence may be regarded as model-independent, as well as to show places where the models differ, and where experiment will be able to tell them apart.

The two models we elect to compare are a fusion model based on work of Das and Hwa,⁹ as applied to hadronic scattering by DeGrand, Duke,

Inami, Miettinen, Ranft and Thacker,^{10,11} and a Bethe-Salpeter model based on work of Blankenbecler and Brodsky.⁶

A. A Fusion Model

It has recently been observed by Ochs that the x_F ($= 2p_{||}/\sqrt{s}$ in the c.m. frame) distributions of fast mesons produced in proton-proton collisions closely resemble the x distributions of partons known from deep-inelastic lepton-nucleon scattering.¹² If these mesons were produced from the fast partons by fragmentation, just as hadrons are produced from quarks in e^+e^- annihilation, the meson spectra would fall much more steeply in x_F than is observed, since one would have to convolute a fragmentation function for mesons out of quarks over a probability distribution for quarks in the proton. This observation led Das and Hwa⁹ to propose that fast mesons are produced in hadronic reactions by the fusion of valence and sea partons, at x_V and x_S , respectively, into a meson at $x_F = x_V + x_S$. (See Fig. 2(a).) Thus the production of fast mesons measures the combined probability for finding two quarks at once in the wave function of the proton:

$$\frac{1}{\sigma} \frac{Ed\sigma}{d^3p} (pA \rightarrow MX) = \int F_{VS}(x_V, x_S) R^M \left(\frac{x_V}{x}, \frac{x_S}{x} \right) dx_V dx_S \quad (2.1)$$

where σ is the nondiffractive pA cross section, F_{VS} the diparton probability distribution--the correlated probability that parton V has momentum fraction x_V , and parton S a fraction x_S of the proton's momentum, and $R^M(x_V/x, x_S/x)$ is a recombination function which parametrizes the fusion of the quark and antiquark into M. R can be decomposed into a two-body piece and a many-body piece

$$R^M \left(\frac{x_V}{x}, \frac{x_S}{x} \right) = R_2 \left(\frac{x_V}{x}, \frac{x_S}{x} \right) \delta(x - x_V - x_S) + \bar{R}(x_V, x_S) \quad (2.2)$$

Because of the difficulty of many-body recombination, the many-body component \bar{R} only becomes competitive for x near 1, where it gives rise to Regge behavior. The two quarks of the two-body component R_2 carry the valence quantum numbers of the meson M .

The situation is only slightly more complicated in the case of production of a fast meson from the target in a reaction induced by a pointlike trigger. Here one measures the combined probability for seeing three partons in the wave function of the proton (Fig. 2(b)). It is customary to measure a differential cross section normalized with respect to the pointlike cross section. For instance, the meson spectrum in the target fragmentation region in deep-inelastic electron-hadron scattering is

$$\begin{aligned}
 F(x_{Bj}, x_F^*) &= \frac{d\sigma}{d^3 p_e d^3 p_\pi} \frac{1}{\frac{d^3 p_e}{E_e}} \\
 &= \frac{\sum_{i,a,b} e_i^2 \int F_{iab}(x_{Bj}, x_a, x_b) R(x_a, x_b) dx_a dx_b \Big|_{x_a+x_b=(1-x_{Bj})x_F^*}}{\sum_i e_i^2 F_i(x_{Bj})}
 \end{aligned}
 \tag{2.3}$$

where e_i is the charge of the i th parton, x_F^* is the fraction of the recoiling core's momentum (in the infinite momentum frame) carried off by the meson, and a and b run over all allowed valence and sea partons. Similar expressions apply to neutrino-induced deep-inelastic scattering and to inclusive production with an associated Drell-Yan pair, and will be given in Sections III and IV.

So far the discussion has been quite general. In order to make predictions for inclusive hadron spectra, however, it is necessary to

make models for the multi-quark distributions in the target. The authors of Ref. 10 have written down a Kuti-Weisskopf model for the nucleon wave function. In this model the proton's parton distribution is assumed to consist of a sum of terms, each of which contains three valence partons and n sea partons (quarks, antiquarks, or gluons)

$$\begin{aligned}
 dP &= Z(P) \sum_n dP_n \\
 dP_n &= \prod_{i=U,U,D} f_{V_i}(x_i) \frac{dx_i}{x_i} \\
 &\cdot \frac{1}{n_1! n_2! n_3! n_4!} \prod_{j=0}^{n_1} f_{\text{sea},1}(x_j) \prod_{j=0}^{n_2} f_{\text{sea},2}(x_j) \\
 &\cdot \prod_{j=0}^{n_3} f_{\text{sea},3}(x_j) \prod_{j=0}^{n-\sum n_i} f_{\text{sea},4}(x_j) \prod_{j=1}^n \frac{dx_j}{\sqrt{x_j^2 + \frac{\mu^2}{p^2}}} \\
 &\cdot \delta \left(1 - \sum_{i=1}^3 x_i - \sum_{j=1}^n x_j \right) \tag{2.4}
 \end{aligned}$$

where the $f_{V,i}$'s are the matrix elements for the valence quarks, the $f_{\text{sea},j}$'s are those for the sea partons (up, down, and strange quarks, and gluons) and $Z(P)$ is a normalization factor. One then calculates an N -parton distribution by integrating over the $n-N$ unseen partons in dP_n and summing on n .

The particular form of the multiparton distribution depends on the choice of the f_V 's and f_{sea} 's. The authors of Ref. 10 selected

$$\begin{aligned}
 f_u(x) &= x^{1-\alpha_0} \\
 f_D(x) &= x^{1-\alpha_0} (1-x) + 3.5(1-x)^2
 \end{aligned}$$

$$f_{\text{sea},i}(x) = g_i^2 (1-x)^{n_i} \quad (2.5)$$

with $\alpha_0 = 1/2$ and

$$g_u^2 = g_{\bar{u}}^2 = g_d^2 = g_{\bar{d}}^2 = .1375$$

$$g_s^2 = g_{\bar{s}}^2 = 9.5 \cdot 10^{-3}$$

$$g_{\text{glue}}^k = 3.36 \quad (2.6)$$

$$n_u = n_{\bar{u}} = n_d = n_{\bar{d}} = 6.8$$

$$n_s = n_{\bar{s}} = 1.2$$

$$n_{\text{glue}} = 2.7 \quad (2.7)$$

These matrix elements are chosen to give valence quark distributions which behave as $x^{-1/2}$ for small x (consistent with Regge behavior) and sea distributions $\sim 1/x$ at small x . In general, multiparton distributions behave like

$$F_{ijk\dots}(x_i, x_j, x_k, \dots) = f_i(x_i) f_j(x_j) f_k(x_k) \dots \phi_{n_s}(1 - \sum x_i) \quad (2.8)$$

where

$$\phi_{n_s}(1-X) = R(X) (1-X)^{g^2 - 1 + n_s(1-\alpha_0)} \quad (2.9)$$

with $g^2 = \sum g_i^2$ and n_s is the number of spectator valence quarks in the reaction: $n_s = 3$ for $F_{\text{sea}}(x)$ or $F_{\text{sea sea}}(x_1, x_2)$, $n_s = 2$ for $F_u(x)$ or $F_{u,s}(x_u, x_s)$, and so forth. These counting rules arise because measuring the X near 1 behavior of a collection of partons measures the X near zero behavior of the spectators, which vanishes like $x^{1-\alpha_0}$ for valence spectators and x^0 for sea spectators. $R(X)$ is finite and nonvanishing for all X .

The model has been applied to a combination of deep inelastic and hadronic single particle inclusive data in order to determine the parameters of Eqs. (2.6)-(2.7). The fragmentation function is taken to be the simple form

$$R_2(\xi_1, \xi_2) = \text{constant} \cdot \xi_1 \xi_2 \quad (2.10)$$

With a broad range of parameters it is easy to fit νW_2 over the entire range of x and single meson spectra for $x_F \geq 0.5$ or so. Additional assumptions are needed to extend the single meson spectra below $x=0.5$ however. Here the physical picture of hadron production becomes rather complicated, with contributions present from sea-parton-sea-parton fusion, resonance decay, gluon fusion, quark fragmentation, and the like. A simple prescription which the authors of Ref. 10 found convenient in extending their analysis of the data was to enhance sea-sea fusion over valence-sea fusion by a factor (determined by explicit fitting) of 7. Since sea-sea fusion yields a meson spectrum $\sim(1-x)^7$ which is negligible compared to valence-sea fusion $\sim(1-x)^3$ at large x , the nature of the fit for that range of x is unchanged. The set of parameters shown in Eqs. (2.5)-(2.7) provide a good representation of the data, with

$$\nu W_2^{\text{proton}} \sim (1-x)^{3.8}, \quad \nu W_2^{\text{neutron}} / \nu W_2^{\text{proton}} \underset{x \rightarrow 1}{\sim} 1/4 \quad (2.11)$$

and reasonable K and π spectra in $pp \rightarrow \pi^\pm X, K^\pm X$.

In keeping with our aim to provide a minimal extrapolation from hadronic data, we shall adopt the model without changes and apply it to a description of meson spectra produced in the target fragmentation region of reactions initiated by a pointlike trigger.

B. A Model Based on a Bethe-Salpeter Equation

The Kuti-Weisskopf model we have just presented has as its basis a multiparton wave function which makes a strong differentiation between valence quarks and sea quarks. For instance, the $qqqq\bar{q}$ component of the proton's wave function in that model has a probability distribution

$$dP_5 \sim F_V(x_1)F_V(x_2)F_V(x_3) f_S(x_4)f_S(x_5) \prod \frac{dx_i}{x_i} \delta(1-\sum x_i) \quad (2.12)$$

where we have neglected differences in F's due to flavor. While such a structure makes calculations extremely easy, there are no compelling reasons for it to be correct. Indeed, there are models where it is not. Consider, for example, an n-body bound state described by a Bethe-Salpeter equation. There the momentum of the bound state is shared equally among the n partons, each one with $\langle x \rangle \sim 1/n$. Although it is not the language one uses to do the calculations, a Bethe-Salpeter wave function for the proton would show a probability distribution

$$dP = Z(P) \Sigma dP_n$$

$$dP_n \sim \prod_{i=1}^n f_n(x_i) \frac{dx_i}{x_i} \delta(1-\sum x_i) \quad (2.13)$$

i.e., with all the partons in an n-parton component of the nucleon having a similar probability distribution.

It is of interest to attempt to extract phenomenology from a Bethe-Salpeter-like model. To reach that goal we follow the work of Brodsky and Farrar¹³ and Brodsky and Blankenbecler⁶ in their derivation of counting rules for large and small momentum transfer processes.

The Bethe-Salpeter approach is exemplified by the parton model calculation of deep-inelastic scattering, in which the proton is assumed to

break up into a quark (which is struck by the photon) and a recoiling core of n spectators. The differential cross section is given by (see Fig. 3(a)):

$$\begin{aligned} \frac{Ed\sigma}{d^3p} (eN \rightarrow eX) &= \sum_a \frac{1}{s} \int |\psi_N(p_a^2)|^2 |M(ea \rightarrow eb)|^2 \\ &\times d^4p_b d^4p_c dm_c^2 \rho(m_c^2) \\ &\times \delta^+(p_b^2 - m_b^2) \delta^+(p_c^2 - m_c^2) \frac{\delta^4(e+N-e'-p_b-p_c)}{(2\pi)^5} \end{aligned} \quad (2.14)$$

writing the matrix element as an incoherent sum over intermediate states a and integrating over the core mass m_c^2 . The wave function ψ is written in terms of a vertex function

$$\psi_N(p_a^2) = \frac{\phi(p_a^2)}{p_a^2 - m_a^2} \quad (2.15)$$

and the lepton-quark matrix element is

$$|M|^2 = \frac{e^4}{Q^4} \text{Tr } \not{\epsilon} \gamma_\mu \not{\epsilon}' \gamma_\nu \text{Tr } \not{p}_a \gamma_\mu \not{p}_b \gamma_\nu .$$

Defining finite momentum frame variables

$$\begin{aligned} p_N &= \left(P + \frac{M^2}{4P}, \quad \vec{0}_1, \quad P - \frac{M^2}{4P} \right) \\ q &= \left(P - \frac{Q^2}{4P}, \quad \vec{0}_1, \quad P + \frac{Q^2}{4P} \right) \\ p_c &= \left((1-x)P + \frac{M_{c1}^2}{4(1-x)P}, \quad \vec{k}_1, \quad (1-x)P - \frac{M_{c1}^2}{4(1-x)P} \right) \end{aligned} \quad (2.16)$$

with

$$M_1^2 = k_1^2 + M^2$$

so that

$$\frac{d^3 p_c}{2E_c} = \frac{dx}{2(1-x)} d^2 k_\perp$$

we find the usual formula for deep inelastic scattering

$$\frac{Ed\sigma}{d^3 p} (eN \rightarrow eX) = \frac{4\alpha^2}{Q^4} \frac{s^2 + u^2}{s(s+u)} F(x_{Bj}) \quad (2.17)$$

where

$$x_{Bj} = \frac{Q^2}{(s+u)}$$

$$s = (p_e + p_N)^2, \quad u = (p_e, -p_N)^2$$

and

$$F(x) = \frac{x^2}{2(1-x)} \int \frac{d^2 k}{(2\pi)^3} \frac{|\phi(p_a^2)|^2}{(p_a^2 - m_a^2)^2} \rho(m_c^2) dm_c^2 \quad (2.18)$$

From (2.16) we have

$$p_a^2 - m_a^2 = \frac{-1}{1-x} \left[k_\perp^2 + m_a^2(1-x) + m_c^2 x - x(1-x) M^2 \right] \quad (2.19)$$

where upon, writing the vertex function $\phi(k^2) \sim (k^2)^{1-n}$ for large k^2 ,

$$F(x) = \frac{1}{2} x^2 (1-x)^{2n-1} \int \frac{d^2 k_\perp}{(2\pi)^3} \frac{\rho(m_c^2) dm_c^2}{\left[k_\perp^2 + m_a^2(1-x) + m_c^2 x - x(1-x) M^2 \right]^{2n-2}} \quad (2.20)$$

which shows the expected counting rule behavior $((1-x)^{2n-1})$ as $x \rightarrow 1$.

Finally we can perform the k^2 integral to find

$$F(x) = \frac{x^2 (1-x)^{2n-1}}{(4\pi)^2} \int \frac{\rho(m_c^2) dm_c^2}{\left[m_a^2(1-x) + m_c^2 x - x(1-x) M^2 \right]^{2n-1}} \quad (2.21)$$

The $x \rightarrow 1$ behavior of (2.21) is independent of details of $\rho(m_c^2)$. That is not the case as $x \rightarrow 0$. For instance, if $\rho(m_c^2) = \delta(m_c^2 - \mu^2)$, then of

course

$$F(x) = \frac{1}{(4\pi)^2} \frac{x^2(1-x)^{2n-1}}{\left[m_a^2(1-x) + \mu^2 x - x(1-x)M^2 \right]^{2n-1}} \quad (2.22)$$

If the spectrum of core masses is chosen to reflect the Regge behavior of the forward amplitude $\bar{q}N \rightarrow \bar{q}N$, $\rho\left(\frac{m_c^2}{M^2}\right) \sim \left(\frac{m_c^2}{M^2}\right)^\alpha$

$$F(x) \sim x^{1-\alpha} \quad (2.23)$$

In addition, the $x \rightarrow 0$ behavior of $F(x)$ is beset by two additional complications: First, the nucleon wave function is a sum of terms: a three-parton piece, a five parton ($qqq\bar{q}q$) piece, and so forth: the higher parton pieces as well as the qqq piece contribute to $F(x)$:

$$F(x) = \sum_{n_s} (1-x)^{2n_s-1} f_{n_s}(x) \quad (2.24)$$

Their effects are not important at large x but become more so at small s . Secondly, the identification $\phi(k^2) \sim (k^2)^{1-n}$ is only viable for $k^2 \gg m^2$; i.e. (see Eq. (2.19)) for $1-x$ small. So the Bethe-Salpeter approach to $F(x)$ as described here has a simple form only for the large- x behavior of the structure function.

We now turn to semiinclusive deep-inelastic scattering. By straightforward analogy with the previous example let us assume that the nucleon N breaks up into a quark a (which is struck by the virtual photon) and a core b of n_s spectators; the core then breaks up into a meson c and a recoiling core of m_s spectators, d (see Fig. 3(b)). Then the differential

cross section is

$$\begin{aligned} \frac{d\sigma}{\frac{d^3 p'}{E'} \frac{d^3 p_c}{E_c}} &= \frac{1}{(2\pi)^8} \int \frac{|\phi(p_a^2)|^2}{(p_a^2 - m_a^2)^2} |M(ea \rightarrow e'a')|^2 \\ &\times \frac{|\phi(p_b^2)|^2}{(p_b^2 - m_b^2)^2} \rho(m_a^2) dm_a^2 \rho(m_b^2) dm_b^2 \frac{d^3 p_d}{2E_d} . \end{aligned} \quad (2.25)$$

Now define

$$\begin{aligned} p_c &= \left((1-x)zP + \frac{m_{c\perp}^2}{4(1-x)zP}, \vec{k}_{\perp c}, (1-x)zP - \frac{m_{c\perp}^2}{4(1-x)zP} \right) \\ p_d &= \left((1-x)(1-z)P + \frac{m_{d\perp}^2}{4(1-x)(1-z)P}, \vec{k} - \vec{k}_{\perp c}, (1-x)(1-z)P - \frac{m_{d\perp}^2}{4(1-x)(1-z)P} \right) \\ p_b &= \left((1-x)P + \frac{\mathcal{M}_{\perp}^2}{4(1-x)P}, \vec{k}_{\perp}, (1-x)P - \frac{\mathcal{M}_{\perp}^2}{4(1-x)P} \right) \end{aligned} \quad (2.26)$$

with

$$\mathcal{M}_{\perp}^2 = \frac{m_{c\perp}^2}{z} + \frac{m_{d\perp}^2}{1-z}$$

and

$$\frac{d^3 p_d}{2E_d} = \frac{dz d^2 k_{\perp c}}{2(1-z)}$$

so that

$$\frac{d\sigma}{\frac{d^3 p'}{E'} \frac{dp_{c\parallel}}{E_{\parallel}}} = \frac{4\alpha^2}{Q^4} \frac{s^2 + u^2}{s(s+u)} F(x_{Bj}, z) \quad (2.27)$$

with

$$\begin{aligned} \widehat{F}(x, z) = & \frac{x^2 z}{(1-x)(1-z)} \int \frac{d^2 k_1}{(2\pi)^3} \frac{d^2 k_{1c}}{(2\pi)^3} \frac{|\phi_N(p_a^2)|^2}{(p_a^2 - m_a^2)^2} \frac{|\phi_b(p_b^2)|^2}{(p_b^2 - m_b^2)^2} \\ & \times \rho(m_b^2) dm_b^2 \rho(m_d^2) dm_d^2 \end{aligned} \quad (2.28)$$

As before,

$$p_a^2 - m_a^2 = -\frac{1}{1-x} \left[k_1^2 + m_a^2(1-x) + \mathcal{M}^2 x - x(1-x)M^2 \right] . \quad (2.29)$$

Writing

$$\phi_N(p_a^2) \sim (p_a^2 - m_a^2)^{1-n_s}, \quad \phi_b(p_b^2) \sim (p_b^2 - m_b^2)^{1-m_s},$$

we have

$$\begin{aligned} F(x, z) = & \frac{x^2}{4} (1-x)^{2n_s-1} (1-z)^{2m_s-1} \\ & \times \int \frac{d^2 k_1 d^2 k_{1c}}{(2\pi)^6} \rho(m_b^2) \rho(m_d^2) dm_b^2 dm_d^2 \\ & \times \frac{1}{\left[k_1^2 + x \mathcal{M}^2 + m_a^2(1-x) - x(1-x)M^2 \right]^{2n_s}} \frac{z^{2m_s+1}}{\left[(1-z)m_d^2 + z m_c^2 - z(1-z) \left(k^2 - m_b^2 \right) \right]^{2m_s}} \end{aligned} \quad (2.30)$$

a result which is easily interpreted in terms of spectator counting rules as $x \rightarrow 1$, $z \rightarrow 1$: the photon strikes the proton, leaving behind a core of n_s spectators, which then fragments into a meson, leaving behind m_s spectators.

As in the case of $F(x)$ above, one could try to guess forms for $\rho(m_b^2)$, $\rho(m_a^2)$ and try to extend one's results to small x, z . Again, I do not know of any unique way to do this: at too small x or z the masses p_a^2 and p_b^2 become small and the simple treatment given above breaks down.

So we have arrived at a description of semiinclusive deep-inelastic scattering in the target fragmentation region which is valid for large x, z :

$$F(x_{Bj}, x_F^*) \sim \frac{\sum_{n,m} C_{nm} (1-x_{Bj})^{2n-1} (1-x_F^*)^{2m-1}}{\sum_n C_n (1-x_{Bj})^{2n-1}} \quad (2.31)$$

The model would satisfy our criterion of "tracking" directly from purely hadronic fragmentation over to pointlike probe-induced fragmentation if we were to assume suitable behavior for $\rho(b^2)$: In the former case the cross section reduces to the counting rules of Blankenbecler, Brodsky and Gunion⁶:

$$\frac{E}{\sigma_{inel}} \frac{d\sigma}{dp_{\parallel}} = \sum_m d_m (1-x_F)^{2m-1} \quad (2.32)$$

In general, we will be able to predict cross sections of the form of Eqs. (2.31) and (2.32) as well as some isotopic ratios. For instance, we have made no additional dynamical statements about the distributions of u or d quarks in the proton. If we assume that $u(x) \sim d(x)$, the BS model predicts the naive result

$$\frac{\frac{Ed\sigma}{dp_{\parallel}} (pp \rightarrow \pi^+ X)}{\frac{Ed\sigma}{dp_{\parallel}} (pp \rightarrow \pi^- X)} \sim \text{large } x_F^2$$

and

$$\frac{Ed\sigma}{dp_{\parallel}} (pp \rightarrow \pi X) \sim (1-x_F)^3$$

since large x_F meson production involves the 3 parton component of the proton's wave function. To compare with data,² which shows a π^+/π^- ratio varying with x , we average the observed π^+/π^- ratio over x from $x=0.2$ to 0.9 : that average value is about 2.5.

It is generally much more difficult to do detailed phenomenology with this model rather than with the K-W model, because it is ambiguous how to include effects whose theoretical justification is uncertain. For example, it is not clear how one should interpret the experimental fact that $F_u(x) \neq F_d(x)$. For large x and for the three-quark component of the proton's wave function one could impose the SU(6) predictions of Farrar and Jackson,¹⁴ but for small x the 5 and 7 quark contributions should become large. In general, it will prove more economical to use the K-W model for the detailed phenomenology of the next section, and reserve the BS model for more general statements, since many of our predictions involve only simple quark counting or extensions thereof, hence will be the same in any scheme, and are most easily carried out in the K-W model.

The two models appear to have quite different underlying assumptions and seem at first glance to be completely unrelated. This initial impression is, however, not correct but arises because of the different language in which (in either case) many of the underlying assumptions are unstated.

Both models admit to the same physical picture. The nucleon interacts with the pointlike trigger by having a parton knocked out. Then the core (nucleon minus a parton) fragments into a $q\bar{q}$ system, the meson, and a shower of spectators. This picture is explicit in the language of the fusion model and can be seen in the diagrammatic representation of the BS model, Fig. 3. What is not so obvious to both pictures is that for large x_F the shape of the inclusive spectrum is independent of the details of the fusion mechanism and depends only on the large x behavior of the parton distribution functions of the model. This result is explicit in

the BS model (where indeed no mention is ever made of a fusion function) but is obscured by the formalism of the fusion model. It is most easily seen in that model by writing, from Eq. (2.8)

$$F_{iab}(x_i, x_a, x_b) = (1-x_i-x_a-x_b)^{f(n)} f(x_i, x_a, x_b)$$

with $f(n) = g^2 - 1 + n_{\text{val}}(1-\alpha_0)$ and $f(x_i, x_a, x_b)$ finite and nonzero for all x . Writing

$$x_i = x_{Bj}$$

$$x_a = (1-x_{Bj})u$$

$$x_b = (1-x_{Bj})v$$

with

$$u+v = x_F^*$$

decouples the inclusive distribution Eq. (2.3) to give

$$\frac{dN}{dx_F} \propto (1-x_{Bj})^{f(n)} (1-x_F^*)^{f(n)} I(x_{Bj}, x_F^*)$$

where I is finite for x_{Bj} or $x_F^* \rightarrow 1$, and depends on the specific form of fusion function $R_2(\xi_1, \xi_2)$. Thus measurement of meson spectra at large x_F^* provide a direct measurement of the multiparton distribution functions of the nucleon, and can provide important information about the nature of its wave function.

Finally, we should point out that neither of these models makes any statement about the magnitude of meson production via resonance decay. It is well known that at small x_F in hadron-hadron collisions resonances are an important source of π 's and K 's. We may estimate their contribution as follows.

Presumably resonances are formed with the same x_F spectrum as prompt mesons. The decay meson spectrum is calculated by convoluting the meson spectrum from resonance decay (which is flat for $\rho \rightarrow \pi\pi$) over the resonance spectrum. If the resonance spectrum is

$$\frac{Ed\sigma}{d^3p}(\text{res}) \sim C_{\text{res}}(1-x_F)^n$$

then

$$\begin{aligned} \frac{Ed\sigma}{d^3p}(\pi) &\sim C_{\text{res}} \int_{x_F}^1 (1-z)^n dz \\ &\sim \frac{C_{\text{res}}}{n+1} (1-x_F)^{n+1} \end{aligned}$$

which is suppressed at large x_F with respect to prompt production. The normalization of resonance formation with respect to meson formation is a priori unknown.

A recent measurement¹⁵ of the reactions $pp \rightarrow \pi\pi X$, $pp \rightarrow \pi\pi\pi X$ at $\sqrt{s}=53$ and 62 GeV has proven to be most useful in elucidating the magnitude of resonance production vs. prompt π production. It is found that $\pi\pi$ and $\pi\pi\pi$ cross sections are comparable in magnitude and shape to single- π spectra. The $\pi^+\pi^-$ spectra show a ρ peak whose area is small compared to the total $\pi\pi$ cross section. As the data span the range $0.4 < x_F < 0.9$, they indicate that resonance decay is not an important contribution to single- π differential cross sections for fast π 's, and that one can perform adequate phenomenological calculations at large x_F without including resonance effects.

The effects of resonance production on hadron spectra in the context of a fusion model has recently been considered by Roberts, Hwa, and

Matsuda.¹⁶

III. DEEP-INELASTIC SCATTERING

We now begin the discussion of various reactions. Deep-inelastic scattering represents one of the simplest tests of the models developed in the last section. The experimentally measured quantity which is most relevant to our discussion is

$$F(x_F^*) \equiv \int d^2 p^M \frac{dN}{d^3 p^M} \frac{E^M}{E^M} \quad (3.1)$$

where

$$\frac{EdN}{d^3 p} \equiv \frac{\int dy \frac{Ed\sigma}{d^3 p dx_{Bj} dy} (\ell p \rightarrow \ell' MX)}{\int dy \frac{d\sigma}{dx_{Bj} dy} (\ell p \rightarrow \ell' X)} \quad (3.2)$$

with $(\ell, \ell') = (\mu^-, \mu^-)$, (ν, μ^-) or $(\bar{\nu}, \mu^+)$ and $y = E_{\ell'}/E_{\ell}$ in the lab frame.

In the fusion model

$$F(x_F^*) = \frac{\sum_{i,a,b} O_i \int dx_V dx_S R\left(\frac{x_V}{x}, \frac{x_S}{x}\right) F_{iab}(x_{Bj}, x_V, x_S)}{\sum_i O_i F_i(x_{Bj})} \quad (3.3)$$

and O_i is the square of the matrix element of the appropriate current: the square of the quark charge in the case of μ and e beams or the square of the appropriate isospin operator in the case of weak interactions.

For large x_F^* , x_{Bj} , both models predict

$$\begin{aligned} F(x_F^*) &\sim \frac{\sum_i O_i (1-x_{Bj})^{n_B} (1-x_F^*)^{n_F}}{\sum_i O_i (1-x_{Bj})^{n_B}} \\ &\sim (1-x_F^*)^{n_F} \end{aligned} \quad (3.4)$$

Experimentalists typically take x_F^* positive to denote quark fragmentation and negative for target fragmentation. We shall on the other hand adopt the convention that x_F^* is always positive simply to retain the connection with the x_F of hadron-hadron scattering.

A. $\mu^- p \rightarrow \mu^- MX$

Virtual photons couple to the charge of the quark. At low x_{Bj} , photons knock out sea partons, at large x_{Bj} , valence partons. The fastest pions (in the target region) are made up via the fusion of a valence u quark with a sea \bar{d} (π^+) or valence d with a sea \bar{u} (π^-). Thus at low x_{Bj} , the π^+/π^- ratio for fast π 's should be about two, since the photon knocks out sea partons and the core has two fast u's and one fast d. But at large x_{Bj} , the photon prefers to knock out a u quark rather than a d quark by a factor of 8 to 1 ($4/9$ for the square of the charge $\times 2$ u's vs. $1/9 \times 1d$) so that the core is mainly $ud + \text{sea}$. The ratio of fast π^+ 's to fast π^- 's should drop to unity. This should happen in x_{Bj} as soon as the valence parton distribution is comparable in size to the sea parton distribution, by $x_{Bj} \sim 0.1$ or so. A curve of the π^+/π^- ratio predicted by the fusion model is shown in Fig. 4, for x_{Bj} running between zero and 0.5. The data points are from the reaction $pp \rightarrow \pi X$,² which is initiated by the interaction of "wee"- $x_{Bj}=0$ partons, and which the $x_{Bj}=0$ limit of the model reproduced nicely.

The dominant part of the cross section at larger x_{Bj}, x_F^* comes from terms in which the photon scatters off a valence quark, leaving behind two valence spectators (or two spectators, in BS language) which emit a meson. See Fig. 5. In this reaction $n_B=3$ (BS) or $g^2-1+(1-\alpha_0)=3.3$ (fusion model fit) and $n_F=3$ (BS) or 3.3 (fusion). Table I gives predicted n_F of the two models for π^+, π^-, K^+, K^- .

We have chosen to normalize the fusion function of the fusion model to the data of del Pappa et al.³ We see that this model provides a good parametrization of the inclusive π^- data over the available x_F range. The predictions of the model for inclusive π^+, π^-, K^+, K^- reactions at $x_{Bj}=0.3$ are shown in Fig. 6. These curves vary only slightly with x_{Bj} ; in Fig. 7 we show inclusive π^+ spectra at $x_{Bj}=0.1$ and 0.3. These differences are probably unobservable.

The most striking difference between the two models is in the K^- spectrum. In the fusion model, K^- 's are produced from sea-sea fusion with γ^* -valence scattering; i.e., with two valence spectators and $n_F=3.8$. In the BS model the photon leaves a ud diquark core behind which fragments into a K^- and 4 spectators (Fig. 5(b)) or $n_F=7$. The observation of the K^- spectrum will provide an unambiguous test between these models, and hence of the nature of the proton's wave function.

Finally, Fig. 8 shows the ratio $F_{K^+}(x_F^*)/F_{K^-}(x_F^*)$ for various x_{Bj} in the fusion model.

B. $\bar{\nu}_p \rightarrow \mu^+ MX$

This reaction is very similar to the preceding one, since the exchange W^- "sees" only u or \bar{d} quarks. (We set $\theta_{\text{Cabibbo}}=0$ for simplicity.) At low x_{Bj} the π^+/π^- ratio is two; at larger x_{Bj} the W^- removes valence u quarks and the isotopic ratio falls to unity. We illustrate that result in Fig. 9, for the fusion model and present predictions of n_F in Table I.

The predictions of the fusion model agrees well with the $\bar{\nu}_p \rightarrow \mu^+ \pi^- X$ data of Derrick et al.,⁴ as shown in Fig. 10. Note that the normalization has been taken from the $\pi^- p$ fit of Section IV.A and also agrees well with the data.

The reader will notice that the π^+/π^- ratio (Fig. 9) can actually dip below 1 at large x_{Bj}, x_F^* . This happens because of our choice of valence u and d distributions. We have required that the $u_V(x)/d_V(x)$ ratio be large at large x. That requires that the $u_V(x)/d_V(x)$ ratio be small at small x, since valence parton distributions are normalized to

$$\int u_V(x) dx = 2$$

$$\int d_V(x) dx = 1 \quad .$$

Large x_{Bj} corresponds to small momentum in the recoiling core, so that measuring π^+/π^- at large x_{Bj} is equivalent to measuring $u(x)/d(x)$ at small x, which can be less than unity. It will be interesting to see if such effects are observable and to try to use them to measure the correlated distributions of flavor quantum numbers in the proton.

The K^+/K^- ratio for this reaction in the fusion model is shown in Fig. 11.

C. $\nu p \rightarrow \mu^- MX$

The virtual W^+ beam knocks only d or \bar{u} quarks out of the proton. Thus at large x_{Bj} all the fast d quarks will have been removed from the core by the W^+ , leaving none to form a π^- . The π^+/π^- ratio should become enormous, resembling the K^+/K^- ratio in $pp \rightarrow KX$.

At large x_{Bj} , the core momentum, $(1-x_{Bj})P$, is small, and so the π^+/π^- ratio falls a bit as sea partons contribute to π^+ and π^- production. In the fusion model this effect can be seen at $x_{Bj} \sim 0.5$. This will be hard to observe since at large x_{Bj} the energy available to make secondaries is small and formation of specific exclusive channels therefore much more important.

The effect is even more dramatic in the BS model, where $F_{\pi^-}(x_F^*) \sim (1-x_F)^7$ due to the required unfavored fragmentation of the core. It will be easy to differentiate this model from the Kuti-Weisskopf model since the latter's π^- spectrum falls as $(1-x)^{3.8}$. This difference arises from the different counting rules of the two models and is identical to the source of the K^- difference in μp or $\bar{\nu} p$ scattering. We present our predictions for n_F in Table I and graphs of $F(x_F^*)$ for meson spectra (in the fusion model) at $x_{Bj}=0.3$ in Fig. 13. The K^+/K^- ratio in that model is shown in Fig. 14.

IV. INCLUSIVE HADROPRODUCTION WITH A DRELL-YAN TRIGGER

One can also perform semiinclusive meson production in association with a massive lepton pair.⁸ The appropriate pointlike indicator of the reaction in the beam particle is a quark in the target projectile; it removes a quark from the target by annihilating it. The properly normalized cross section for semiinclusive hadron production is

$$F(x_F^*, x_F, \tau) \equiv \int d^2 p_M \frac{EdN}{d^3 p_M} \quad (4.1)$$

$$\frac{EdN}{d^3 p_M} = \frac{\sum_{iab} e_i^2 F_{(ib)}(x_2) \int dx_V dx_S R\left(\frac{x_V}{x}, \frac{x_S}{x}\right) F_{ibs}(x_1, x_V, x_S)}{\sum_{iab} e_i^2 F_{(ia)}(x_2) F_{(ib)}(x_1)} \quad (4.2)$$

where the dimuon has a longitudinal momentum fraction x_F of the beam particle and $\tau = M_{\mu^+\mu^-}^2/s$. The sum on i, a, b is understood to be restricted; a and b must be a flavor-antiflavor complimentary pair but can be either valence or sea partons. x_1 and x_2 satisfy the familiar relations

$$\begin{aligned} x_1 x_2 &= \tau \\ x_1 - x_2 &= x_F \end{aligned} \quad (4.3)$$

or

$$\begin{aligned}
 x_1 &= \frac{x_F}{2} + \sqrt{\left(\frac{x_F}{2}\right)^2 + \tau} \\
 x_2 &= -\frac{x_F}{2} + \sqrt{\left(\frac{x_F}{2}\right)^2 + \tau}
 \end{aligned}
 \tag{4.4}$$

The relevant scaling variable which runs from zero to 1 is $x_F^* = x_F^M / (1-x_1)$, where $x_F^M = 2p^M / \sqrt{s}$ is a light cone momentum of the meson M, as the core has a momentum $(1-x_1)\sqrt{s}/2$ after "losing" a quark at $x_1\sqrt{s}/2$ to the annihilation.

Two interesting examples of hadronic production with a Drell-Yan trigger are $pp \rightarrow \mu^+ \mu^- MX$ and $p\bar{p} \rightarrow \mu^+ \mu^- MX$. We may consider several kinematic domains, where the behavior of isotopic ratios will be quite different.

Consider first $x_F=0$, so $x_1=x_2=\sqrt{\tau}$. If τ is small, dilepton production is dominated by sea parton-sea parton annihilation and meson spectra and isotopic ratios should resemble those seen in ordinary hadronic reactions. However, once τ rises above 0.01 or so, valence-valence annihilation (if allowed, if not, valence-sea annihilation) will dominate. In $p\bar{p} \rightarrow \mu^+ \mu^- hX$, $u\bar{u}$ annihilation is 16 times as likely as $d\bar{d}$ annihilation. The resulting final state will be a ud core recoiling against a $\bar{u}\bar{d}$ core, so that the π^+/π^- ratio in either the p or \bar{p} fragmentation region will collapse from two to unity.

The π^+/π^- ratio will also fall in pp collisions as well because of increased depletion of the fast valence u quarks but the effect need not be nearly so pronounced as in the case of $p\bar{p}$ since there are no valence \bar{u} 's present to annihilate.

Now consider $x_F \neq 0$. If x_F is positive, the dilepton and meson move in the same direction in the c.m. of the system. In that case x_1 is driven to a large value but x_2 is small. Valence-sea annihilation dominates tending to leave behind a ud ($\bar{u}\bar{d}$) core from the p (\bar{p}), or $F_{\pi^+}(x_F^*)/F_{\pi^-}(x_F^*) \rightarrow 1$. The spectra will be similar to those seen in $pp \rightarrow \mu^+ \mu^- \pi X$ at $x_F=0$, which is also dominated by valence-sea annihilation.

If x_F is negative, so that the dilepton moves backwards and the meson forwards, sea-valence annihilation wins out. If τ is small the meson spectra should be identical to those in ordinary hadron-hadron scattering, which are also initiated by interactions in the sea. If τ is also large x_1 and x_2 can be both nonzero and the isotopic ratios will resemble those of $p\bar{p}$ reactions at large τ , $x_F=0$.

These features may be seen explicitly in the Kuti-Weisskopf model. Figures 15 and 16 show the π^+/π^- ratios at $x_F=0$ for the reactions $pp \rightarrow \mu^+ \mu^- \pi^\pm X$ and $p\bar{p} \rightarrow \mu^+ \mu^- \pi^\pm X$. In both cases the proton fragments the π . It will be much easier to do the latter experiment with a \bar{p} beam and a p target, rather than vice versa. In that case the isotopic ratios are reversed:

$$F_{p \rightarrow \pi^+}(x_F^*)/F_{p \rightarrow \pi^-}(x_F^*) = F_{\bar{p} \rightarrow \pi^-}(x_F^*)/F_{\bar{p} \rightarrow \pi^+}(x_F^*) \quad (4.5)$$

Figures 17 and 18 show the corresponding ratios at $x_F=0.1$ and -0.1 for several τ 's. The qualitative features noted above are clearly evident in the predictions of the model.

The K^+/K^- ratios in p fragmentation are, as usual, large since $p \rightarrow K^+$ is "favored" fragmentation and $p \rightarrow K^-$ unfavored. We present our predictions at $x_F=0$ for various τ in Figs. 19 and 20.

Finally, the spectra predicted by the model are shown in Figs. 21 and 22 at $x_F=0$, $\tau=0.1$. The eye cannot detect a great deal of difference among spectra at different x_F and τ , so I will not show plots there. The π^+ , π^- , and K^+ spectra fall like $(1-x_F^*)^{3.3}$, the K^- at about $(1-x_F^*)^{3.8}$. The Bethe-Salpeter model of Section II would predict $n_F \sim 3$ and 7 respectively. So once again the crucial differentiation between the models will come from the K^- spectrum. It is safe to say that, since the K^- spectrum falls so steeply in the BS model, observation of any K^- tail above $x_F=0.3$ or so will be strong evidence against it.

Finally, what are the experimental criteria for which these predictions are valid? One should see a big change in the meson spectra by $\tau=0.05$ or so. One requires $M_{\mu^+\mu^-} > 4$ GeV or so to avoid the ψ region and to ensure that the Drell-Yan mechanism is operating. That τ and $M_{\mu\mu}^2$ translate into an $s=320$ GeV², within range of a FNAL-SPS type machine (for pp) or a $p\bar{p}$ collider with E_p of a few hundred GeV, $E_{\bar{p}}$ of a few tens of GeV.

Of course, there are two interesting regions of τ : large τ , to see the dramatic differences expected, and small τ , to see the restoration of "hadronic" charge ratios. The second region, of course, provides a stronger constraint on c.m. energy requirements since one still needs large M^2 , small M^2/s . It seems that experiments which can test the expectations of this section are probably feasible.

V. CONCLUSIONS

In the preceding sections we have presented simple parton model predictions for inclusive meson spectra in the target fragmentation region of reactions induced by a pointlike trigger. These predictions

are illustrated by a simple Kuti-Weisskopf model for multiparton distributions, and the rather detailed predictions of that model are compared to the results of a Bethe-Salpeter model.

We have found that experiments which measure the correlated production of a single lepton (in deep-inelastic scattering) or a massive lepton pair and a fast meson emitted in the target fragmentation region in fact measure the correlated probability distribution of several partons in a hadron. Thus these experiments will serve as a probe of such quantities as flavor correlations in the proton: the likelihood, for instance, that if one sees an up quark in the proton with momentum fraction x_1 , one can see a second up quark at x_2 . The information thus gained will be a valuable constraint on possible models of the parton wave function of the proton.

Our predictions are summarized by the statement that as soon as the pointlike trigger removes a parton of light cone momentum fraction $x > 0.1$ or so from a proton, isotopic ratios of fast mesons produced in the fragmentation of the core of the proton will show a dramatic change. This change reflects the new quantum numbers of the valence partons of the recoiling core of the proton. The altered isotopic ratios should be evident for $x_F^* > 0.3$, where x_F^* is the fraction of the core's momentum carried by the meson.

I think that experiments to test these predictions lie well within the realm of feasibility. The energies required are those available in existing accelerators. The biggest problem in a fixed target machine will be to differentiate slow π^+ 's from protons in the target fragmentation region. A Drell-Yan experiment using colliding $\bar{p}p$ rings in the $s = \text{hundreds of GeV}^2$ range would avoid this difficulty.

Both the Kuti-Weisskopf and Bethe-Salpeter models predict the altered isotopic ratio structure (which is itself nearly only a consequence of quark counting) and shape of the pion spectra. They typically differ in the shape of "unfavored fragmentation" spectra, such as $p \rightarrow K^-$. It would be interesting and useful to measure K^- spectra, or $\nu p \rightarrow \mu^- \pi^- X$, and thus to differentiate between two equally a priori likely models for the distribution of partons in hadrons.

In conclusion, we have seen that experiment already shows that particle production in the target fragmentation region in reactions induced by a pointlike trigger bears much resemblance to purely hadronic fragmentation. Only a little more effort by experimentalists will reveal a rich structure with many dramatic effects which will provide new insights into the distribution of quantum numbers in the proton.

Acknowledgments

This work began as a collaboration with Hannu I. Miettinen, and conversations with him have been invaluable. I would also like to thank him for a critical reading of the manuscript. I would like to acknowledge enjoyable and useful discussions with J. D. Bjorken, R. Blankenbecler, S. Brodsky, D. Duke, and T. Inami. This work is supported by the Department of Energy.

REFERENCES

1. For related discussions see R. P. Feynman, Photon-Hadron Interactions (Benjamin, Reading, MA, 1971); and J. D. Bjorken, Stanford Linear Accelerator Center preprint SLAC-PUB-1756 (1975), unpublished, and Phys. Rev. D 7, 282 (1973).
2. J. R. Johnson et al., Phys. Rev. Lett. 39, 1173 (1977).
3. C. del Pappa et al., Phys. Rev. D 15, 2425 (1977).
4. M. Derrick et al., Phys. Rev. D 17, 1 (1978).
5. J. Kuti and V. F. Weisskopf, Phys. Rev. D 4, 3418 (1971).
6. R. Blankenbecler and S. Brodsky, Phys. Rev. D 10, 2973 (1974) and S. Brodsky and J. Gunion, Phys. Rev. D 17, 848 (1978).
7. See R. P. Feynman (Ref. 1); G. Farrar and J. L. Rosner, Phys. Rev. D 7, 2747 (1973); R. Cahn and E. Colglazier, Phys. Rev. D 9, 2658 (1974); and S. Brodsky and N. Weiss, Phys. Rev. D 16, 2325 (1977).
8. T. DeGrand and H. I. Miettinen, Phys. Rev. Lett. 40, 612 (1978).
9. K. Das and R. Hwa, Phys. Lett. 68B, 549 (1977). Quark fusion as a model for inclusive meson production has also been considered by V. V. Anisovich and V. M. Schekhter, Nucl. Phys. B55, 455 (1973).
10. T. DeGrand, D. Duke, T. Inami, H. I. Miettinen, and H. Thacker, in preparation.
11. Other related applications of the fusion model are, for example, D. Duke and F. Taylor, Phys. Rev. D 17, 1788 (1978) and J. Ranft, Stanford Linear Accelerator Center preprint SLAC-PUB-2052 (1977), submitted to Phys. Rev.
12. W. Ochs, Nucl. Phys. B118, 397 (1977).
13. S. Brodsky and G. Farrar, Phys. Rev. D 11, 1309 (1975).
14. G. Farrar and D. Jackson, Phys. Rev. Lett. 35, 1416 (1976).

15. W. Lockman et al., University of California Los Angeles preprint UCLA-1110a (June 1978).
16. R. G. Roberts, R. C. Hwa, and S. Matsuda, Rutherford Laboratory preprint RL-78-040 (1978).

TABLE I
Particle Spectra

$$\frac{dN}{dx_F^*} = (1-x_F^*)^{N_F}$$

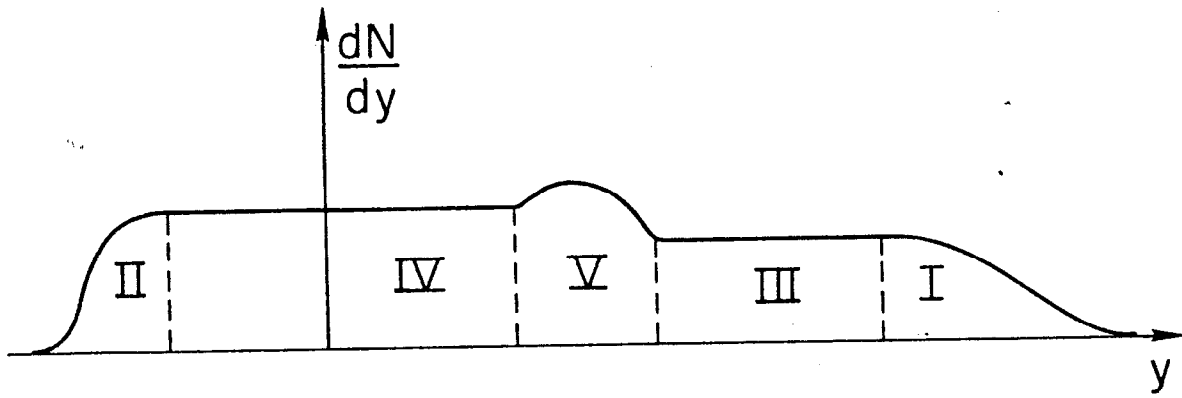
| | <u>Reaction</u> | N_F | | | |
|----|---------------------------------------|---------|---------|-------|-------|
| a) | $\mu^- p \rightarrow \mu^- MX$ | π^+ | π^- | K^+ | K^- |
| | B. S. | 3 | 3 | 3 | 7 |
| | K.W. fusion | 3.3 | 3.3 | 3.3 | 3.8 |
| b) | $\bar{\nu} p \rightarrow \mu^+ MX$ | | | | |
| | B.S. | 3 | 3 | 3 | 7 |
| | K.W. fusion | 3.3 | 3.3 | 3.3 | 3.8 |
| c) | $\nu p \rightarrow \mu^- MX$ | | | | |
| | B.S. | 3 | 7 | 3 | 7 |
| | K.W. fusion | 3.3 | 3.8 | 3.3 | 3.8 |
| d) | $pp \rightarrow \mu^+ \mu^- MX$ | | | | |
| | B.S. | 3 | 3 | 3 | 7 |
| | K.W. fusion | 3.3 | 3.3 | 3.3 | 3.8 |
| e) | $p\bar{p} \rightarrow \mu^+ \mu^- MX$ | | | | |
| | B.S. | 3 | 3 | 3 | 7 |
| | K.W. fusion | 3.3 | 3.3 | 3.3 | 3.8 |

"B.S. and K.W. fusion" refer to the two models of Sections II.B and II.A, respectively.

FIGURE CAPTIONS

1. Schematic dN/dy for the reaction $\gamma^*p \rightarrow hX$, showing the quark fragmentation region I, and the target fragmentation region II, the quark and target central regions III and IV, and the hole region V.
2. Meson production in the fusion model for the reactions (a) $pp \rightarrow MX$ or (b) $\gamma^*p \rightarrow MX$.
3. The Bethe-Salpeter model: (a) deep-inelastic scattering; (b) deep-inelastic scattering followed by target fragmentation.
4. The ratio $F_{\pi^+}(x_F^*)/F_{\pi^-}(x_F^*)$ in the fusion model for the reaction $\mu^-p \rightarrow \mu^- \pi X$ at various x_{Bj} . Data points are for the reaction $pp \rightarrow \pi X$ (Ref. 2).
5. The dominant contributions to meson production in the Bethe-Salpeter model: (a) π^+, π^-, K^+ ; (b) K^- .
6. $F(x_F^*)$ for the reaction $\mu^-p \rightarrow \mu^- hX$, $h = \pi^+, \pi^-, K^+, K^-$, at $x_{Bj}=0.1$. π^- data from Ref. 2.
7. $F_{\pi^-}(x_F^*)$ for $\mu^-p \rightarrow \mu^- \pi^- X$ at $x_{Bj}=0.1$ and 0.3.
8. $F_{K^+}(x_F^*)/F_{K^-}(x_F^*)$ for the reaction $\mu^-p \rightarrow \mu^- KX$ in the fusion model at various x_{Bj} . Data points are for the reaction $pp \rightarrow KX$ (Ref. 2).
9. $F_{\pi^+}(x_F^*)/F_{\pi^-}(x_F^*)$ for the reaction $\bar{\nu}p \rightarrow \mu^+ \pi X$.
10. $F(x_F^*)$ for the reaction $\bar{\nu}p \rightarrow \mu^+ hX$, $h = \pi^+, \pi^-, K^+, K^-$. π^- data from Ref. 3.
11. $F_{K^+}(x_F^*)/F_{K^-}(x_F^*)$ for $\bar{\nu}p \rightarrow \mu^+ \pi X$.
12. $F_{\pi^+}(x_F^*)/F_{\pi^-}(x_F^*)$ for the reaction $\nu p \rightarrow \mu^- \pi X$.
13. $F(x_F^*)$ for the reaction $\nu p \rightarrow \mu^- hX$, $h = \pi^+, \pi^-, K^+, K^-$, in the fusion model.

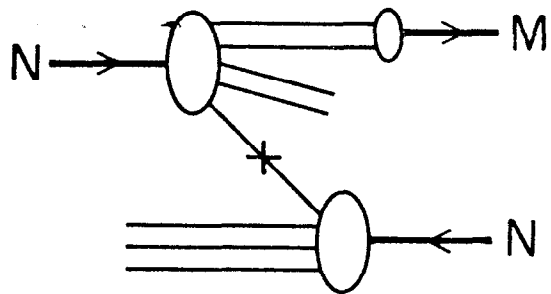
14. $F_{K^+}(x_F^*)/F_{K^-}(x_F^*)$ for $\nu p \rightarrow \mu^- K X$ in the fusion model.
15. $F_{\pi^+}(x_F^*)/F_{\pi^-}(x_F^*)$ for $pp \rightarrow \mu^+ \mu^- \pi X$ at $x_F=0$.
16. $F_{\pi^+}(x_F^*)/F_{\pi^-}(x_F^*)$ for $p\bar{p} \rightarrow \mu^+ \mu^- \pi X$ at $x_F=0$.
17. $F_{\pi^+}(x_F^*)/F_{\pi^-}(x_F^*)$ for $pp \rightarrow \mu^+ \mu^- \pi X$ for nonzero τ and x_F .
18. Same as Fig. 17, but for $p\bar{p} \rightarrow \mu^+ \mu^- \pi X$.
19. $F_{K^+}(x_F^*)/F_{K^-}(x_F^*)$ for $pp \rightarrow \mu^+ \mu^- K X$ at $x_F=0$.
20. Same as Fig. 19, but for $p\bar{p} \rightarrow \mu^+ \mu^- K X$.
21. $F(x_F^*)$ for $pp \rightarrow \mu^+ \mu^- h X$, $h = \pi^+, \pi^-, K^+, K^-$.
22. Same as Fig. 21, but for $p\bar{p} \rightarrow \mu^+ \mu^- h X$.



8-78

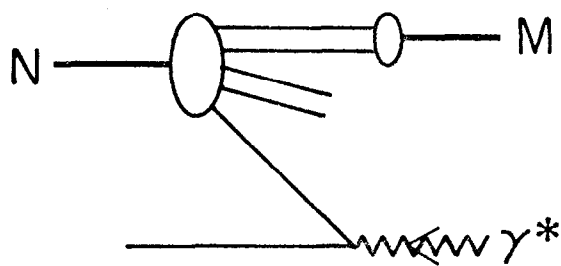
3461A1

Fig. 1



8-78

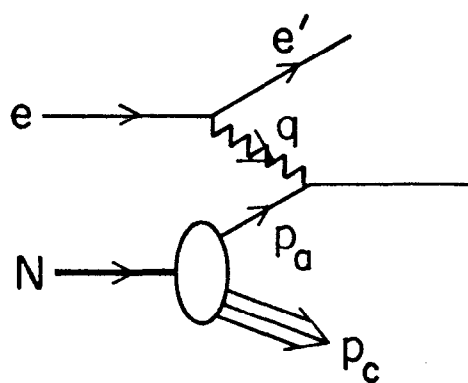
(a)



3461A2

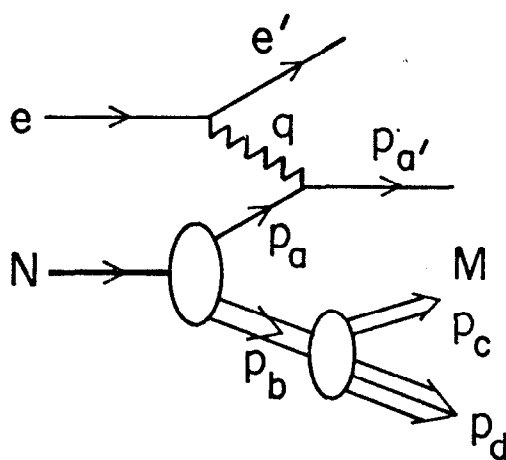
(b)

Fig. 2



8-78

(a)



3461A3

(b)

Fig. 3

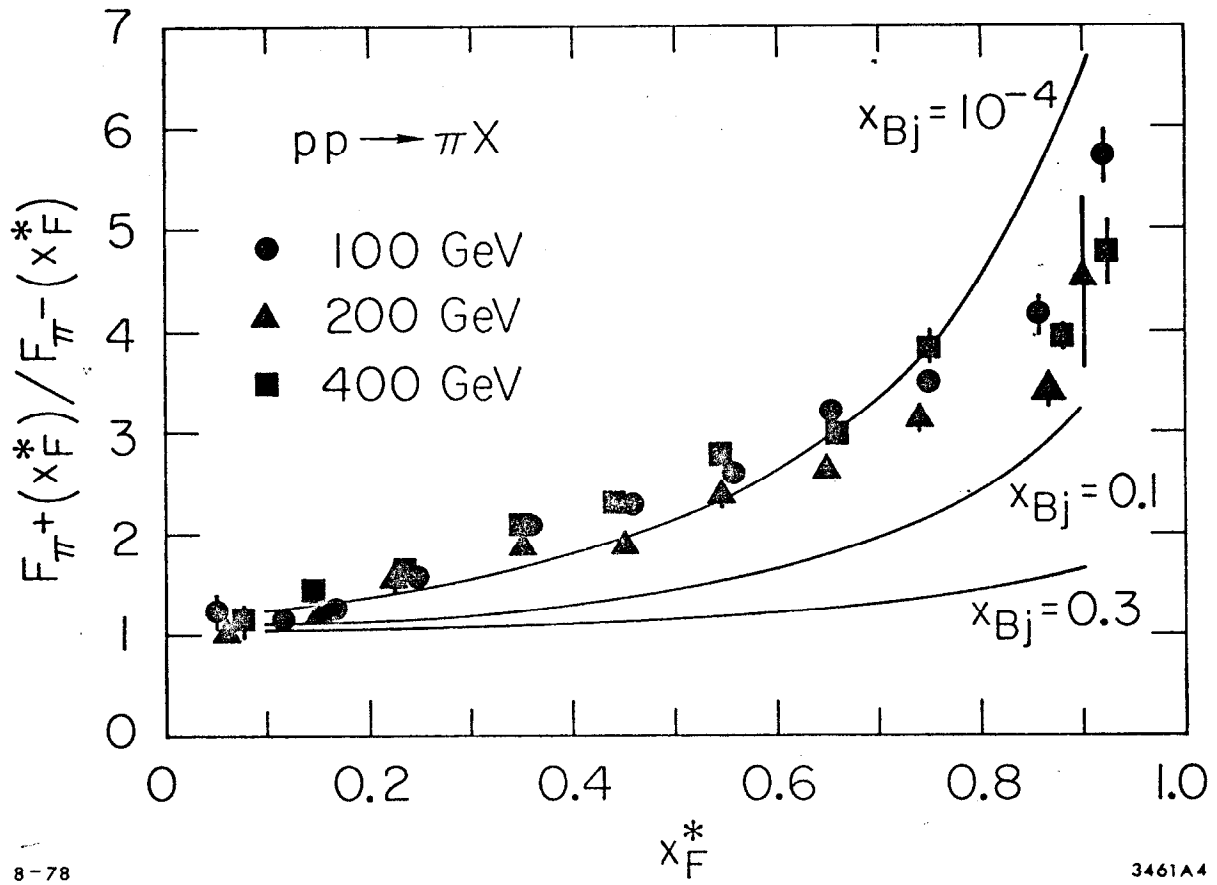
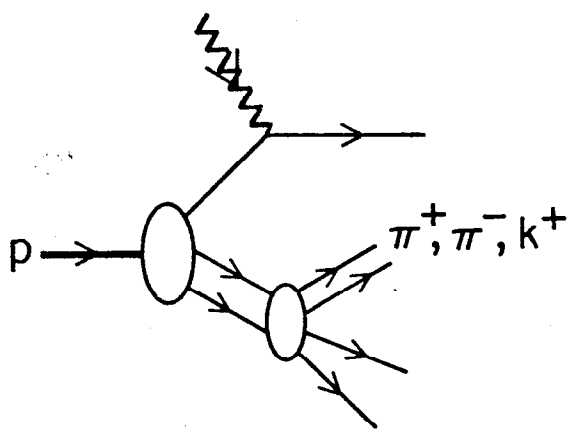
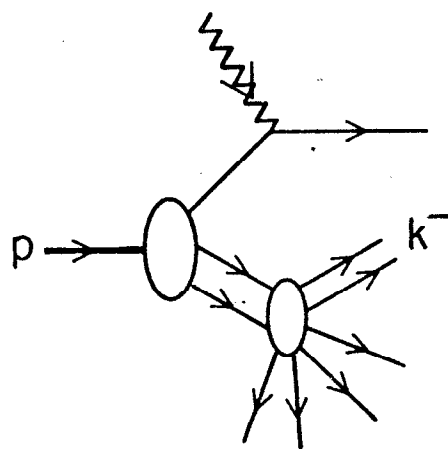


Fig. 4



8-78

(a)



(b)

3461A5

Fig. 5

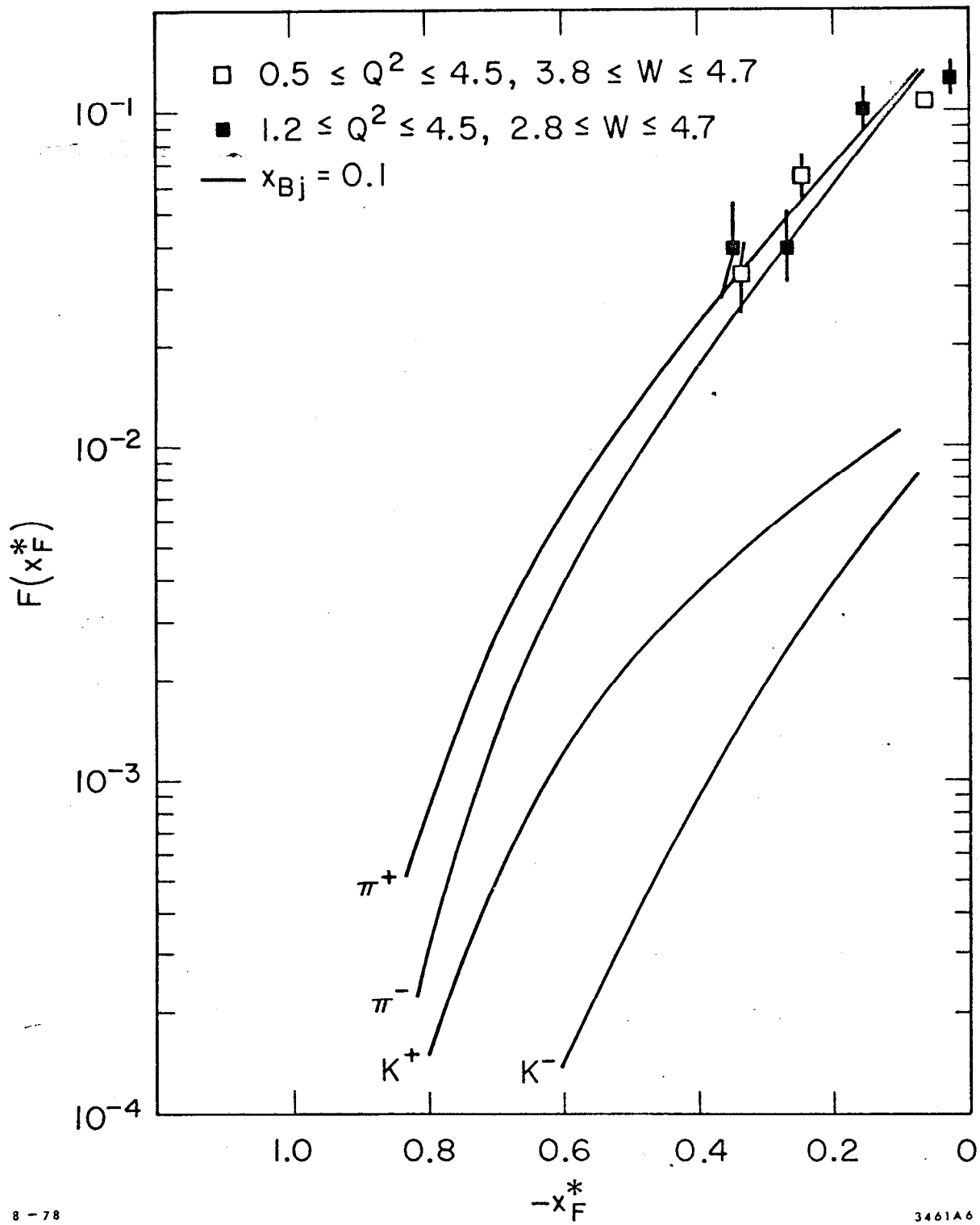


Fig. 6

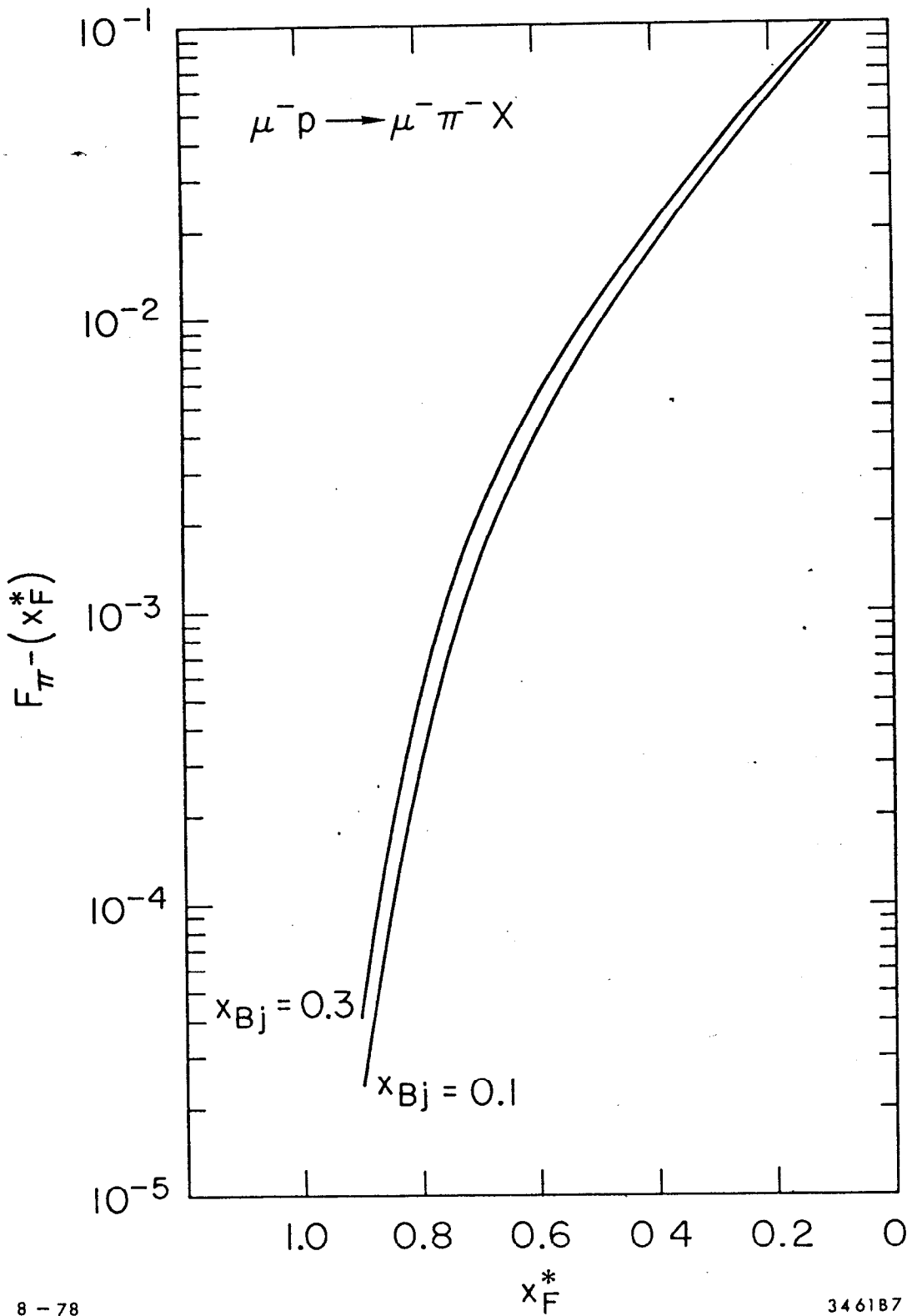


Fig. 7

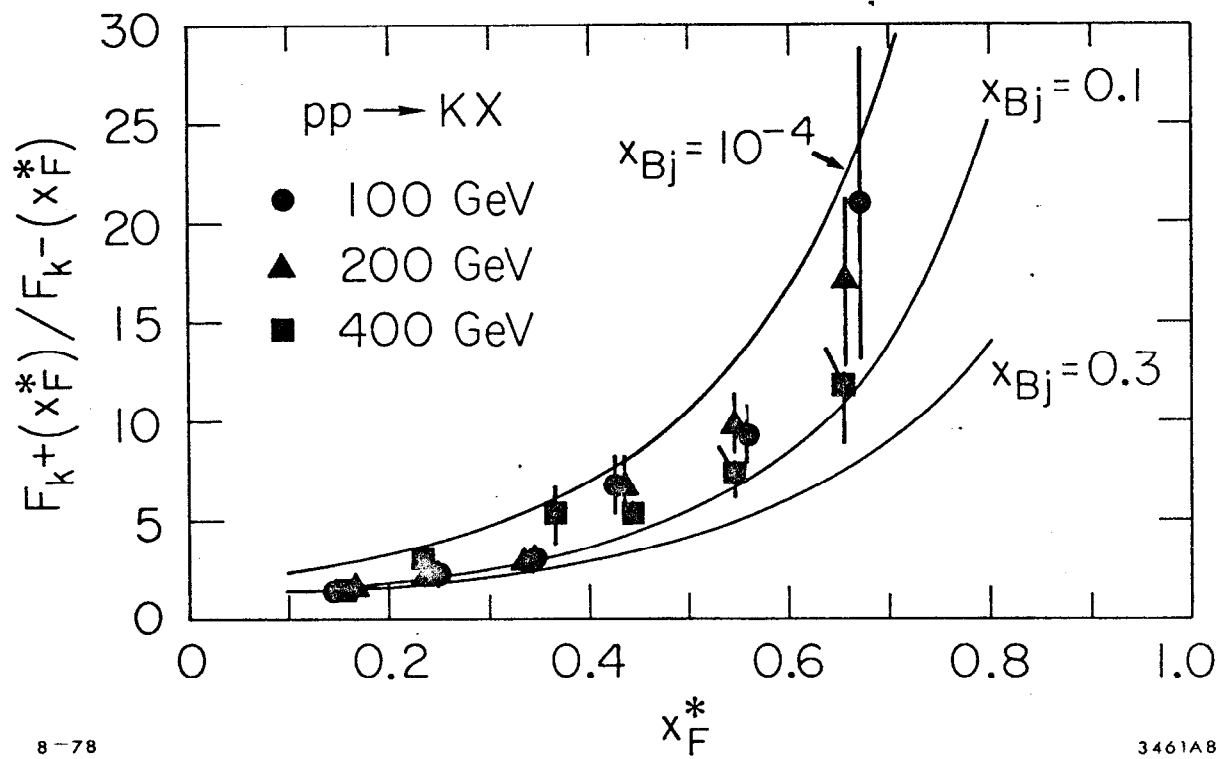


Fig. 8

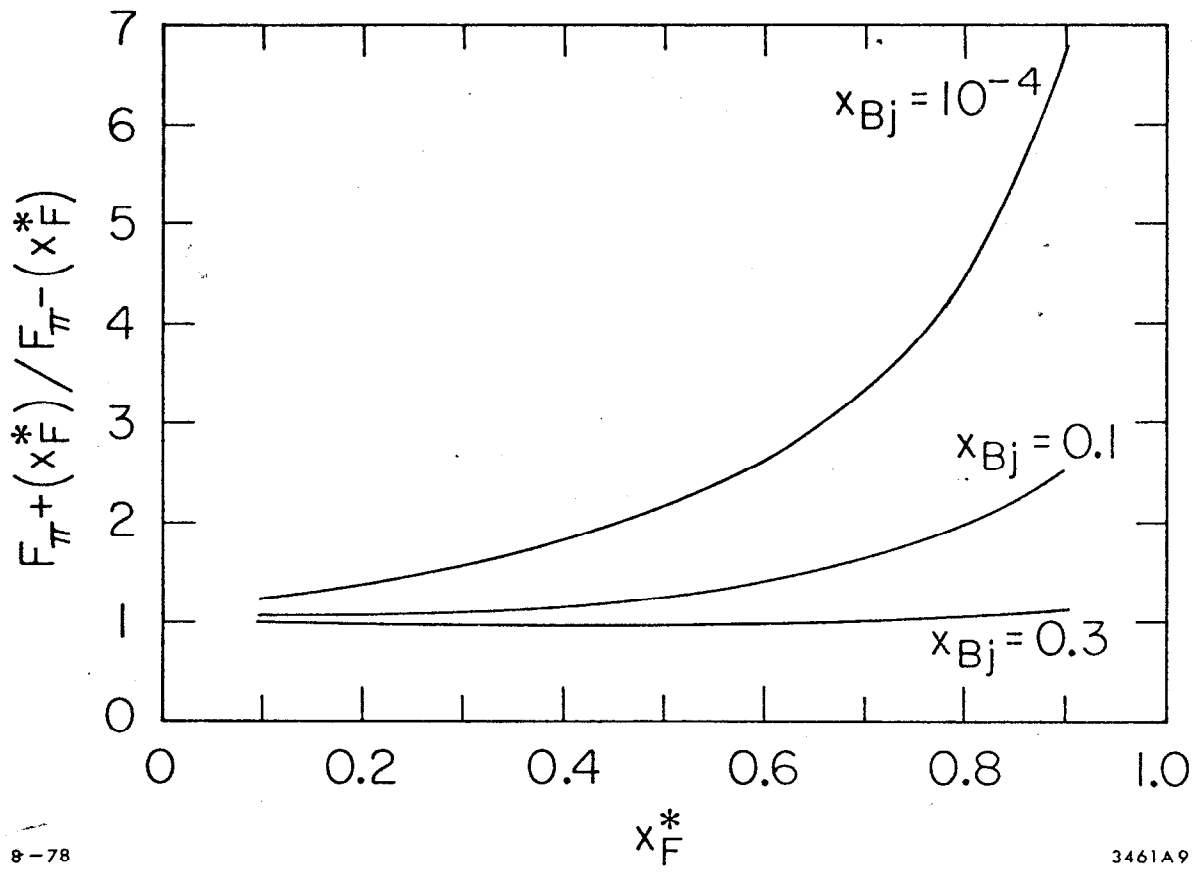


Fig. 9

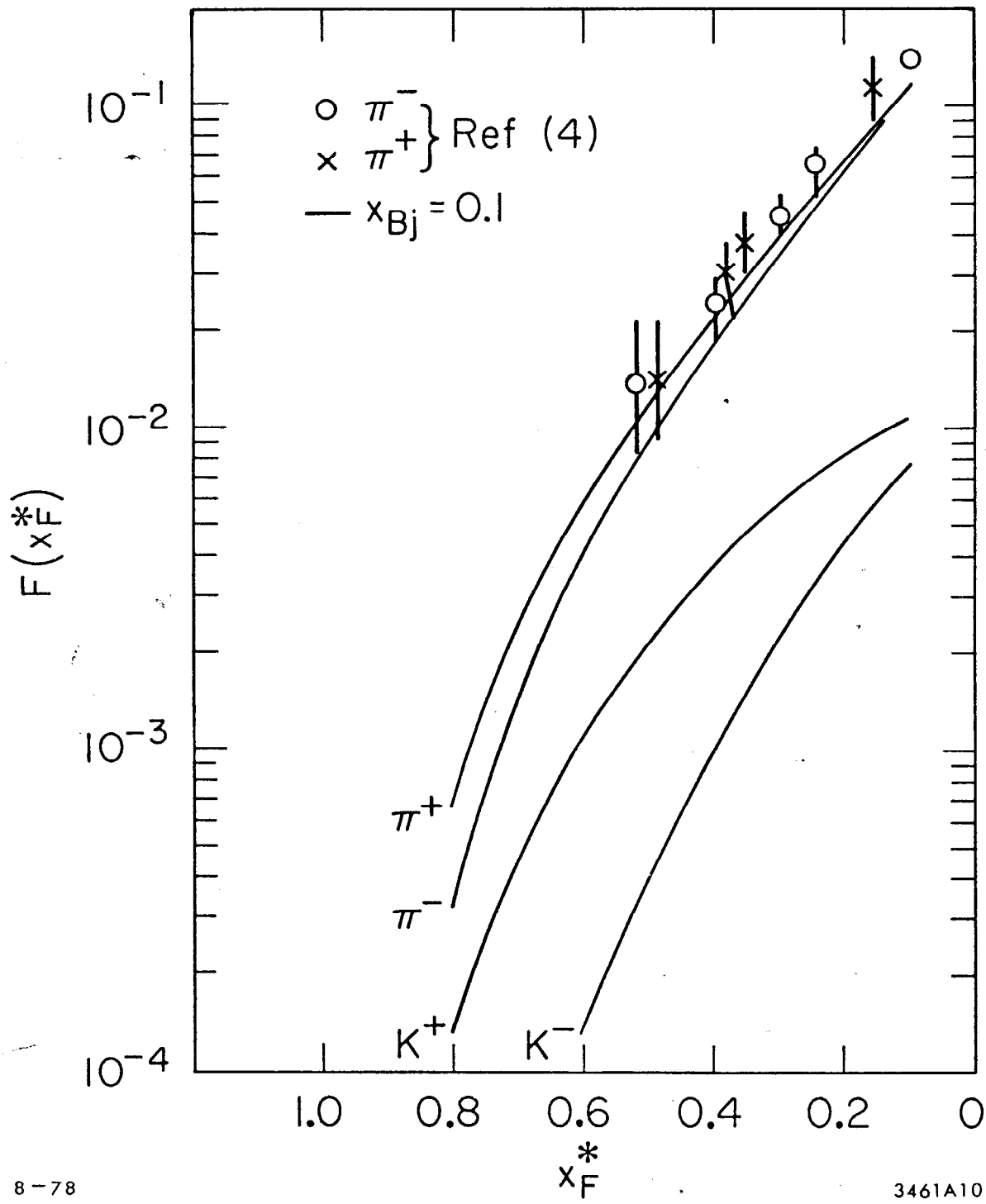


Fig. 10

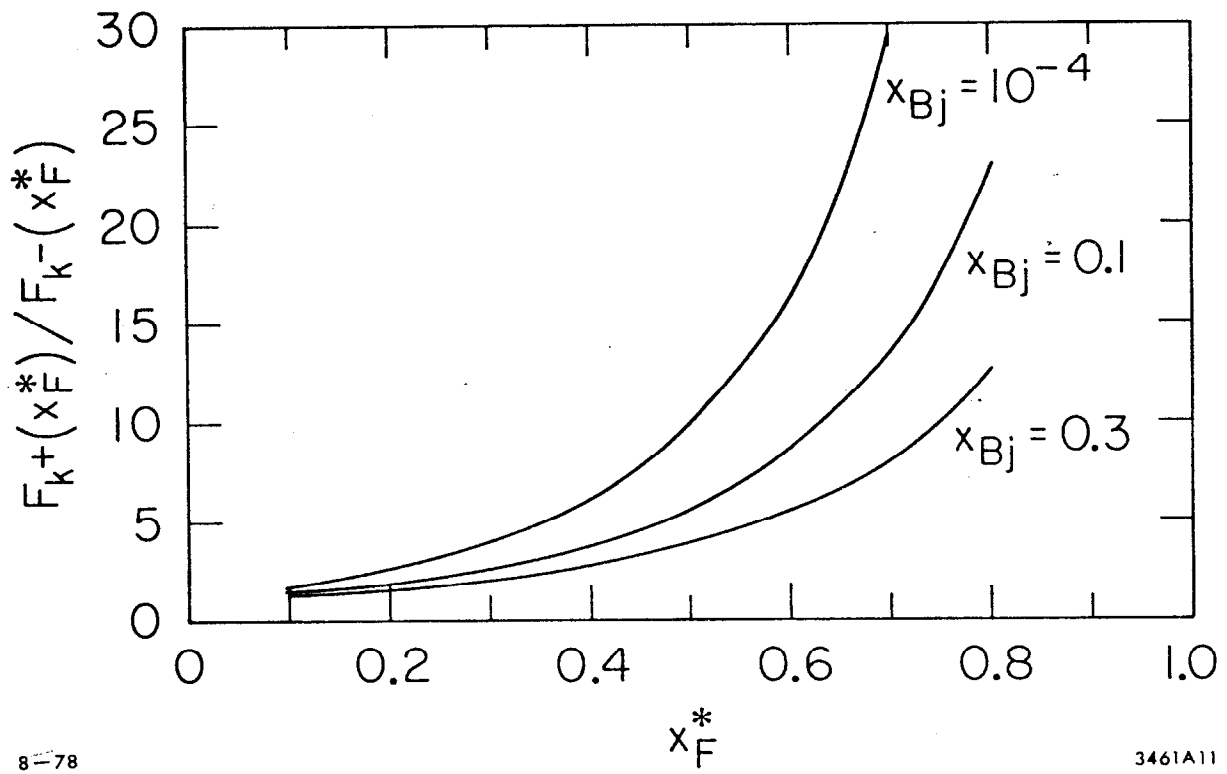
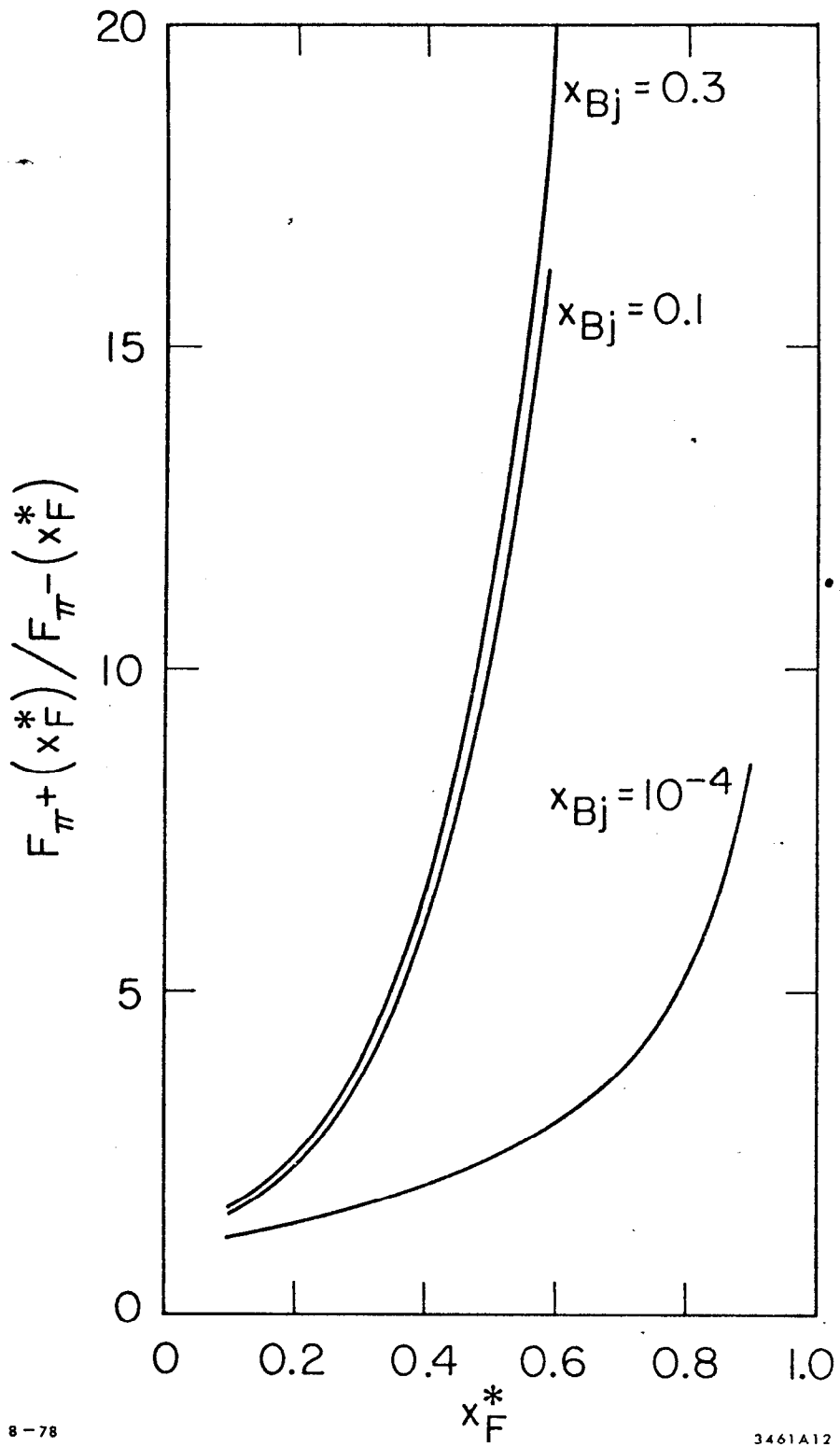


Fig. 11



8-78

3461A12

Fig. 12

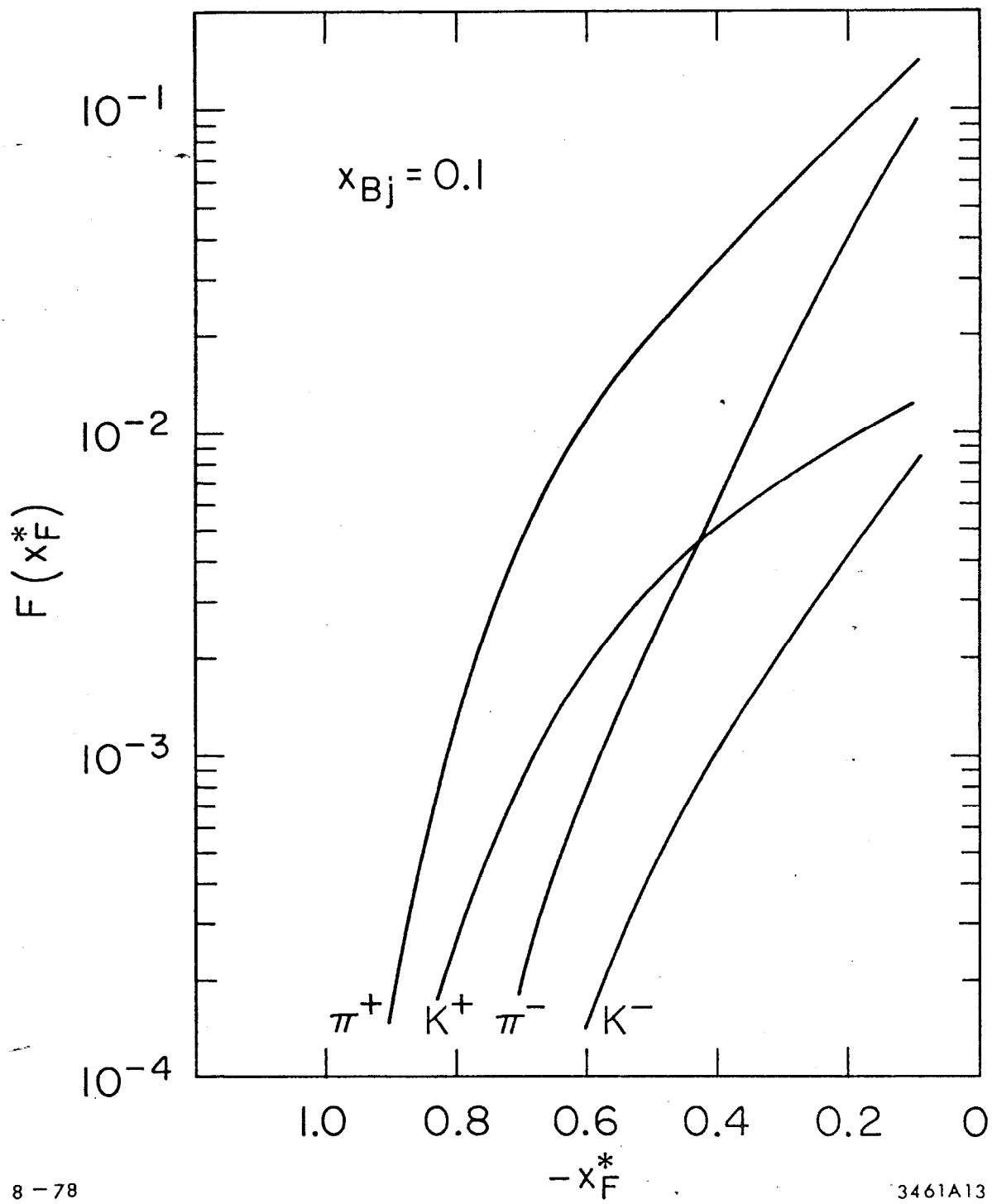


Fig. 13

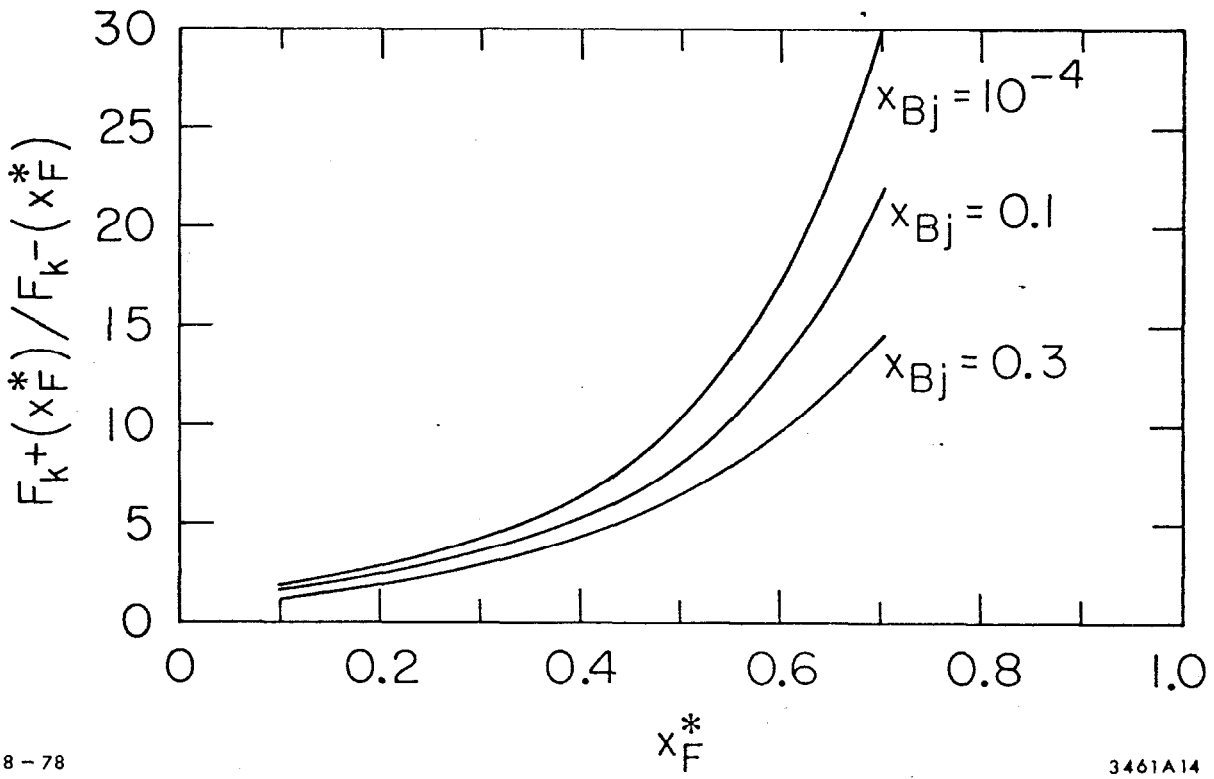
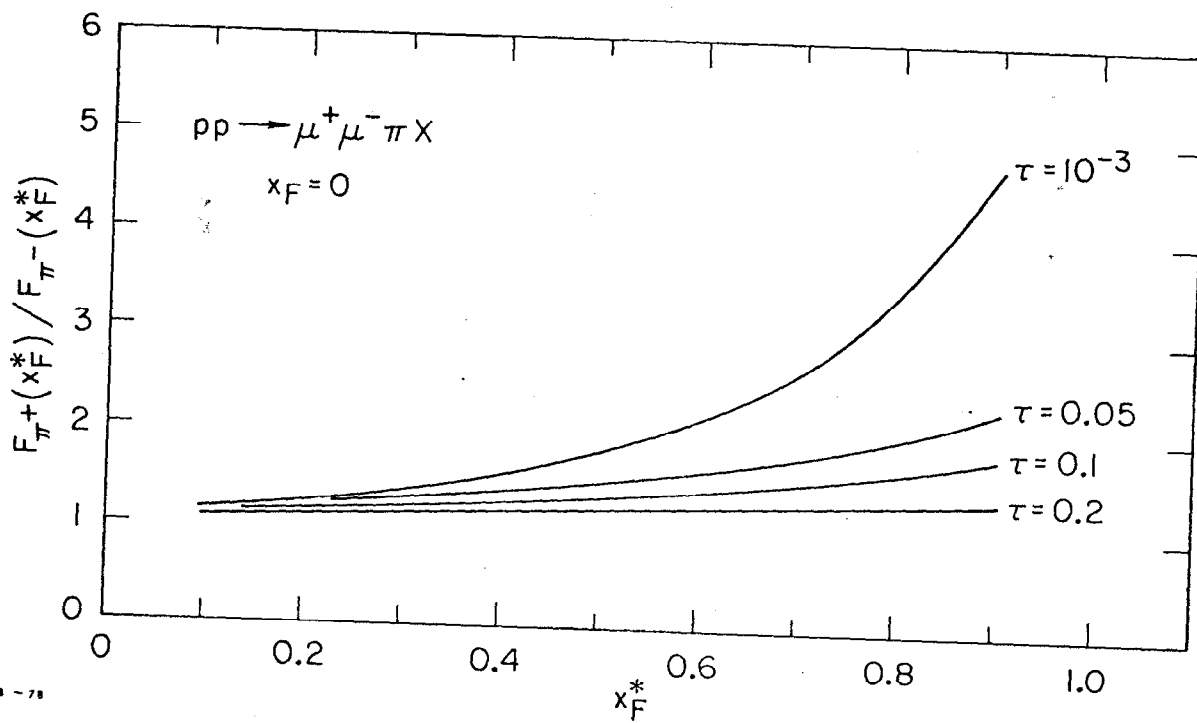


Fig. 14



3461A15

Fig. 15

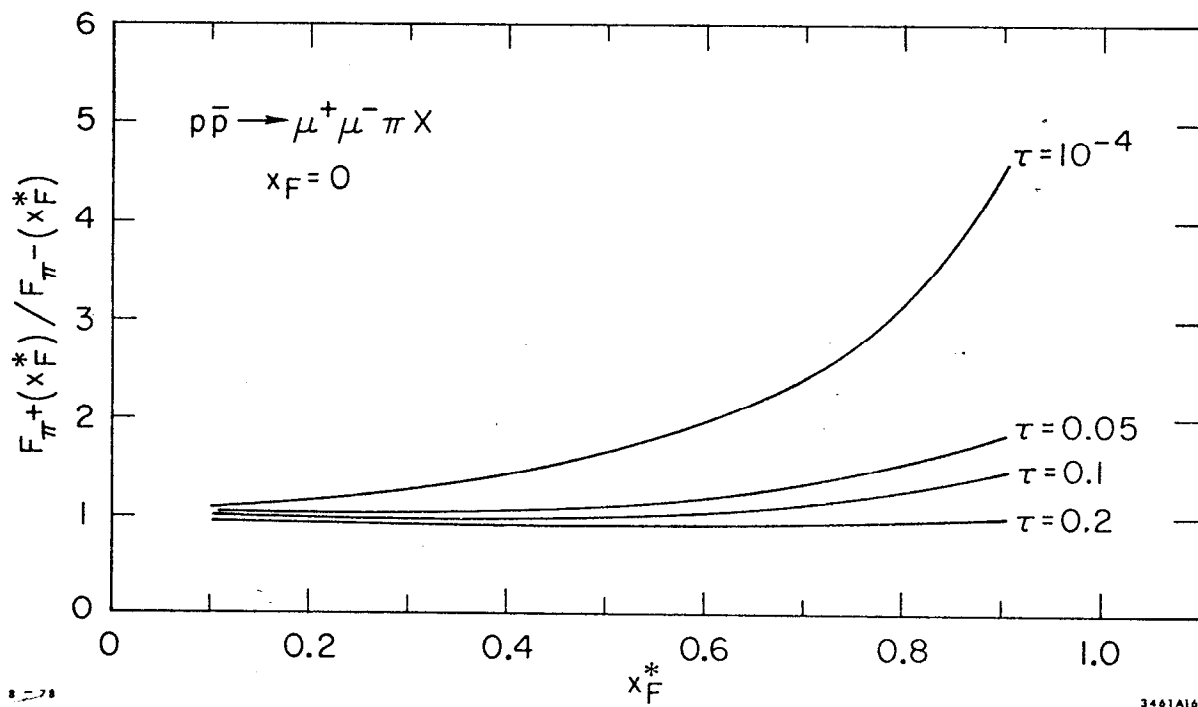


Fig. 16

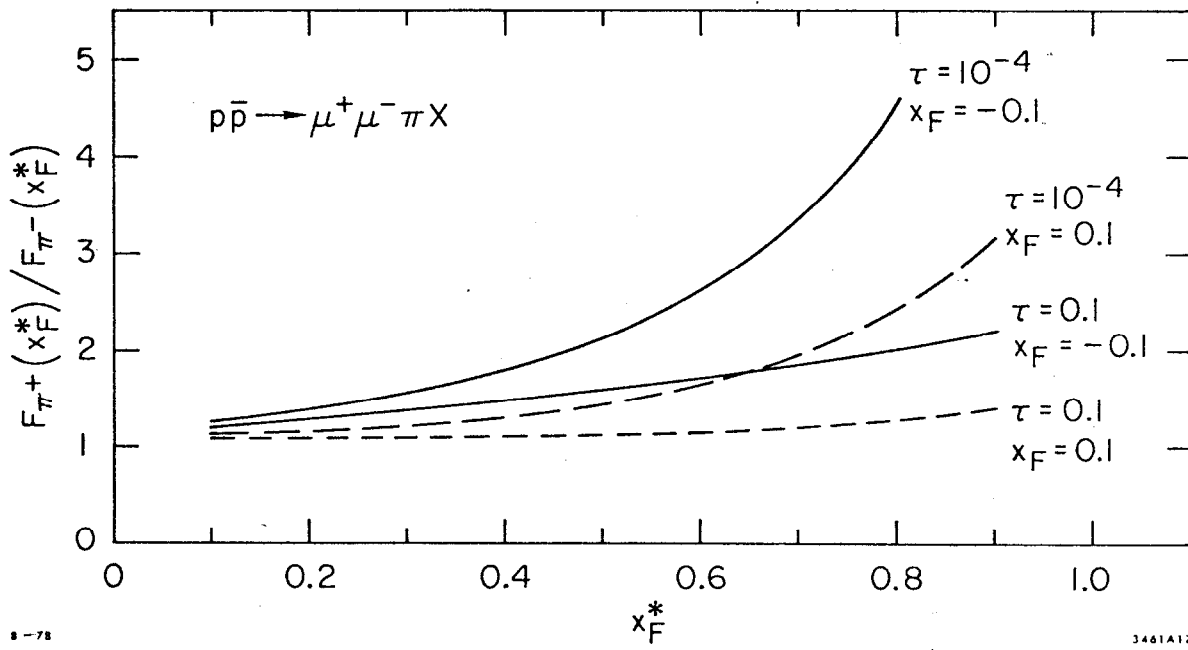


Fig. 17

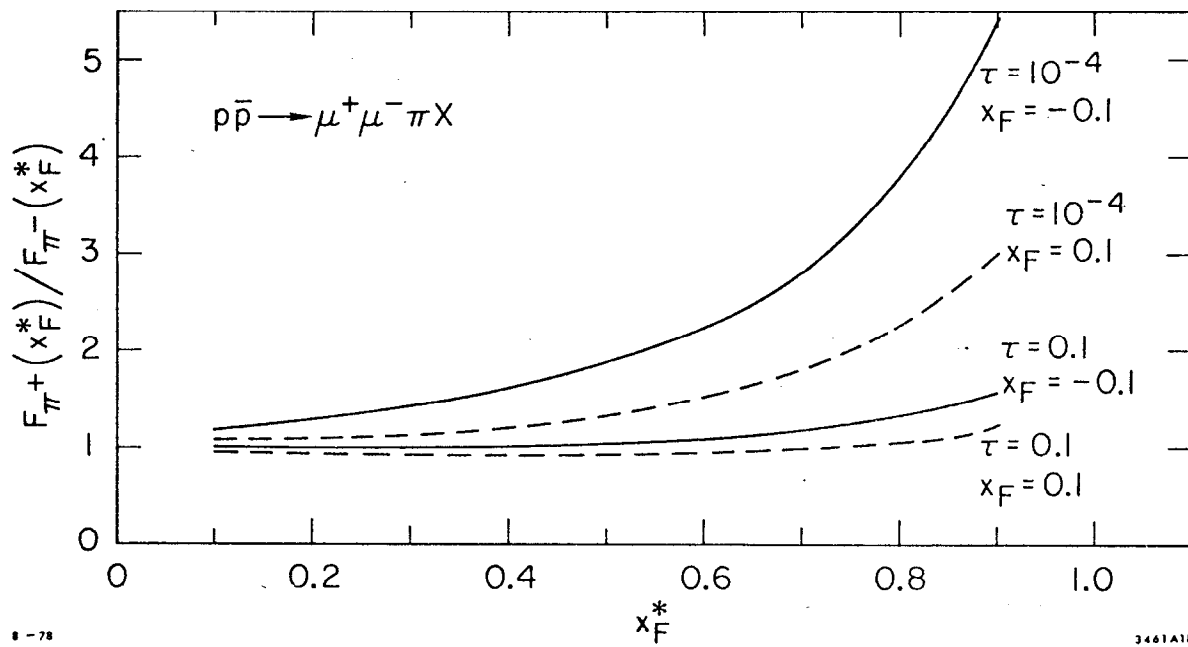


Fig. 18

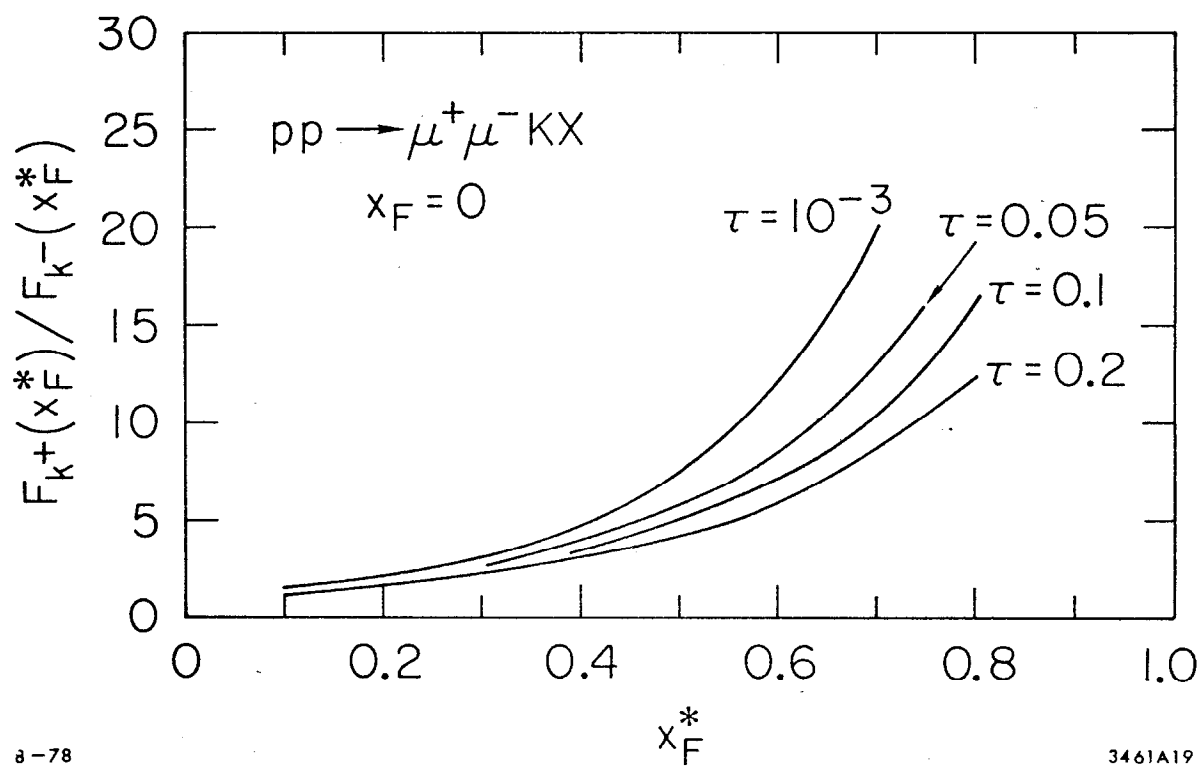


Fig. 19

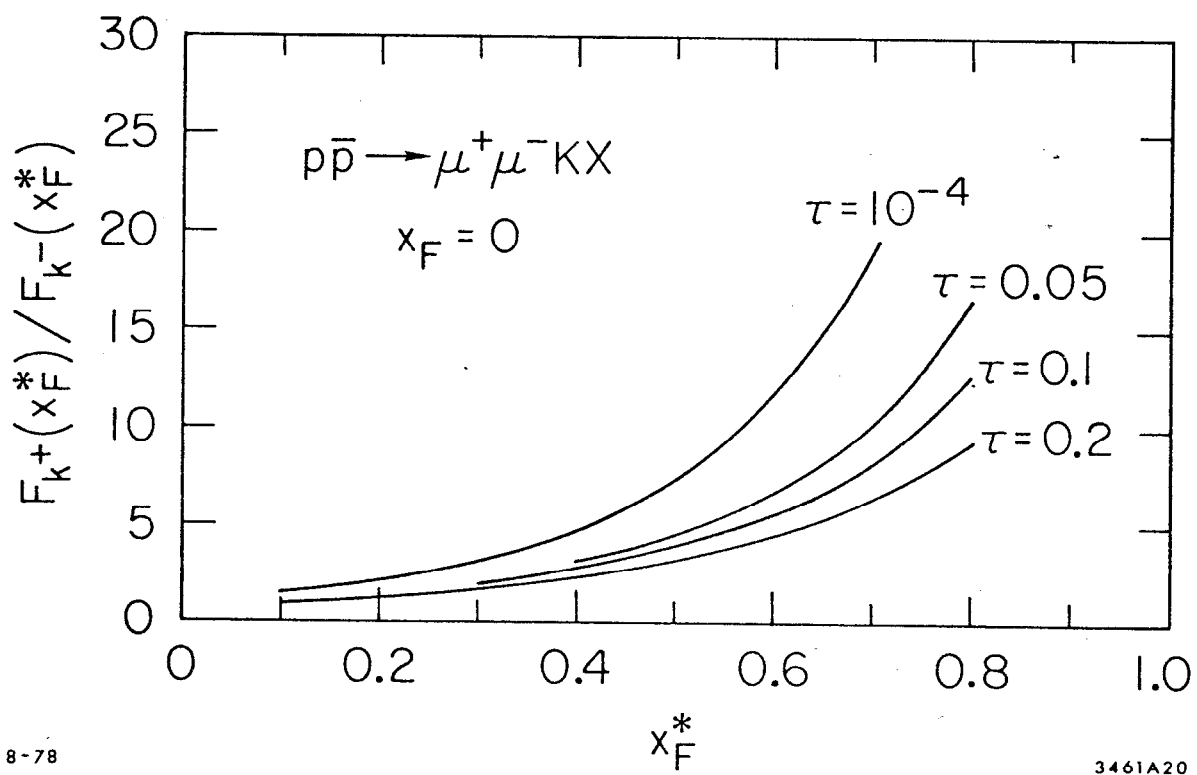


Fig. 20

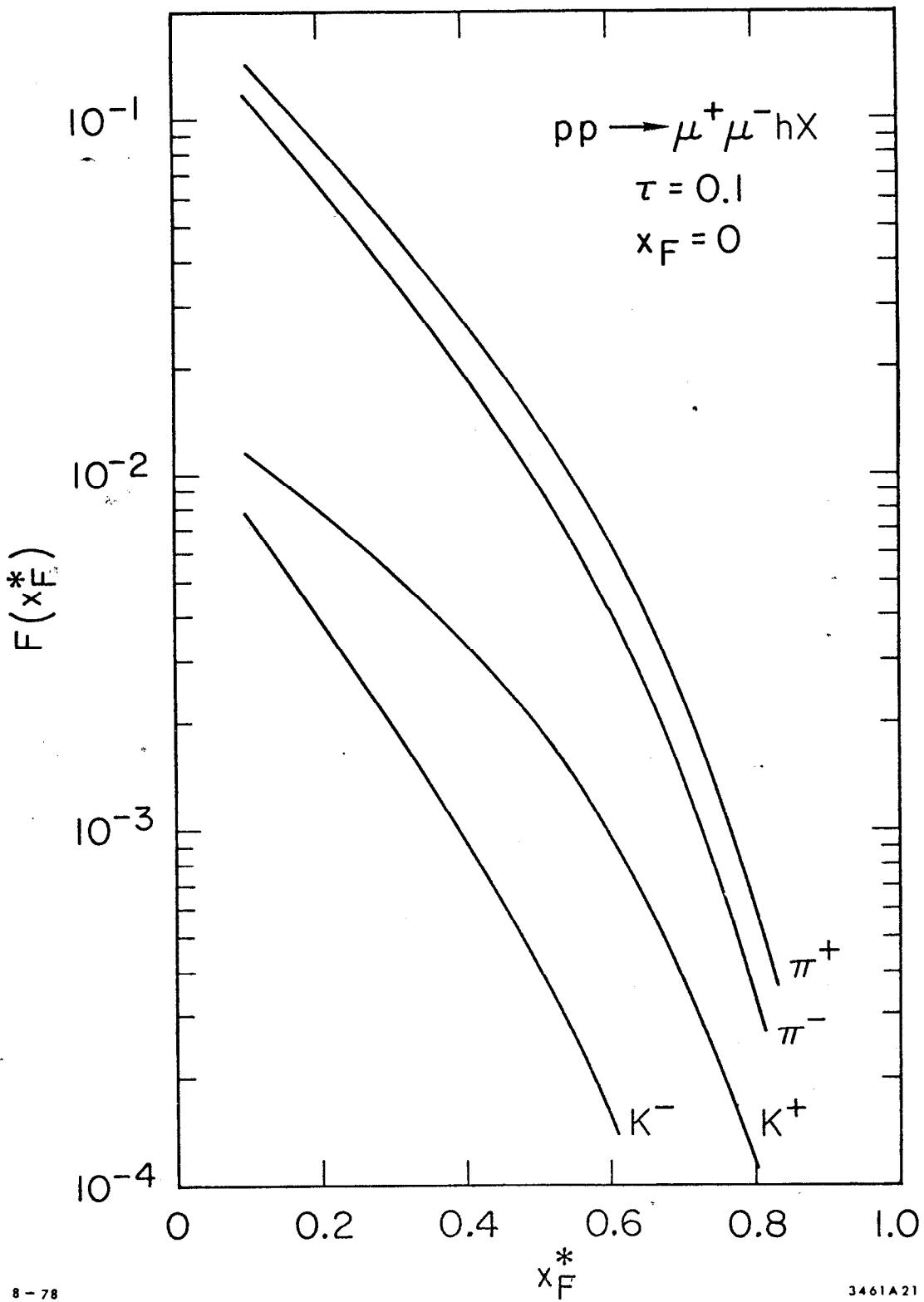


Fig. 21

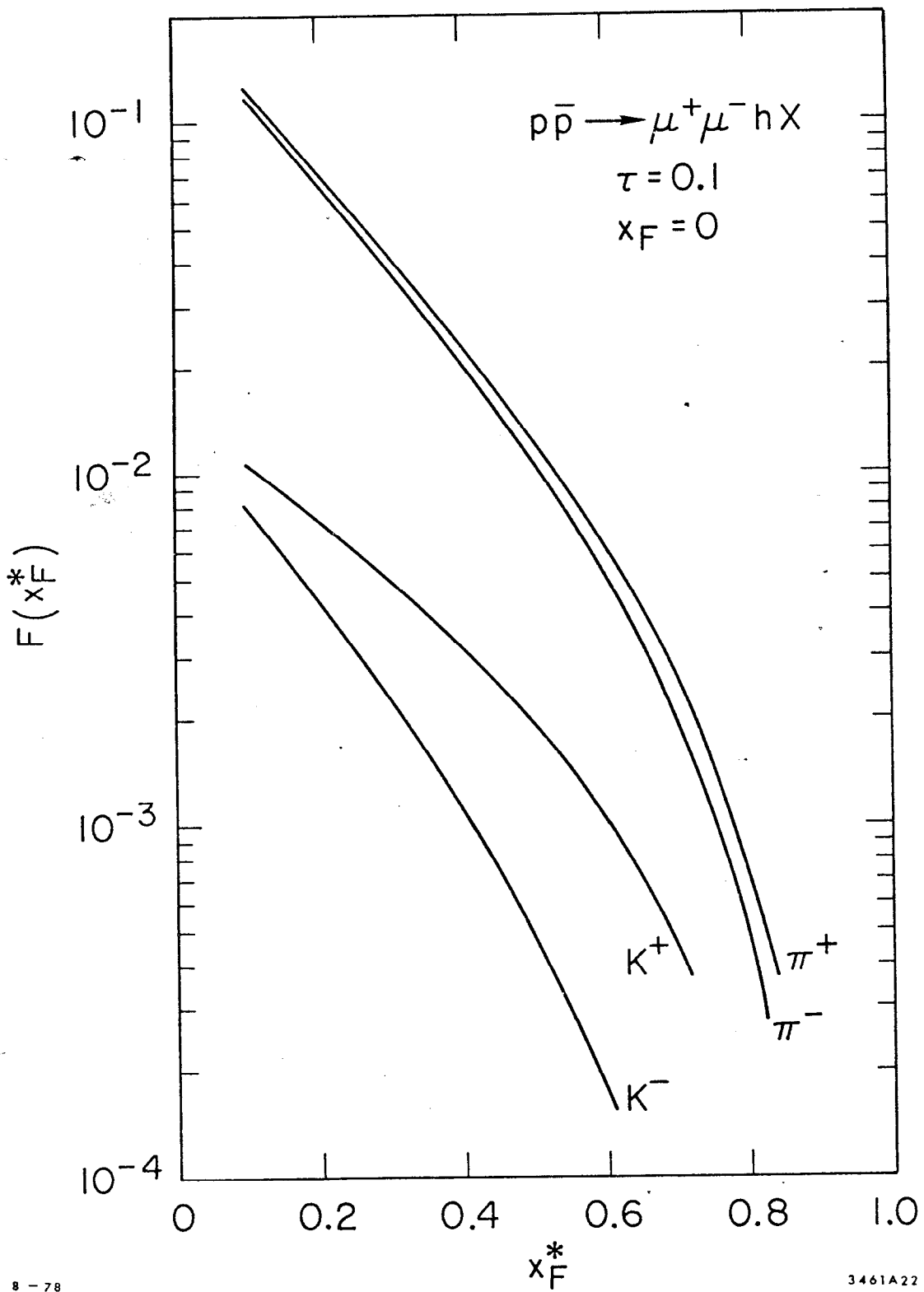


Fig. 22